Hydraulic modeling of flow, water levels and inundations: Serein River case study

Firas S. M. SALEH (1*), Agnès DUCHARNE(1), Ludovic OUDIN(1), Nicolas FLIPO(2) et Emmanuel LEDOUX(2)

(1) Laboratoire UMR-CNRS Sisyphe, Université Pierre-et-Marie-Curie, 4 place Jussieu, 75252 Paris, France.

(2) Centre de Géosciences, Mines ParisTech, UMR Sisyphe, 77305 Fontainebleau, France.

* firas.saleh@upmc.fr

1 Introduction

The main objective of this thesis is to contribute to a better simulation of floods in the hydrographic network of the Seine, and their links with inundations, wetlands and stream-aquifer interactions including the contribution of the groundwater to low flows, and the reinfiltration of water in storage areas after floods.

More specifically, contributing to the development of a hydraulic module, allowing the simulation of floods and has coupling capabilities with a large scale basin hydrological model MODCOU (Ledoux, 1980).

To facilitate such coupling, the first part of this thesis aims at establishing whether a reliable hydraulic flood routing model could be developed based on limited field data. A wide variety of "what if" river geometry scenarios are explored to determine the most appropriate river representation geometry in areas where cross sections surveys are not available.

The validity of this approach has been illustrated by developing a model of the Serein River (tributary of the Yonne River).

The modelization methodology is based on the association between a hydraulic and hydrological model. The hydraulic model used is HEC-RAS which is based on the Saint Venant equations solved by using the four point implicit finite difference scheme. The calibration parameter involved in the development of the hydraulic model is the Manning's roughness coefficient (n). The hydrogeological model MODCOU is used to simulate the lateral inflows of the Serein River subcatchments.

2 River routing literature review

Flood routing has long been of vital concern to man as he has sought to understand, construct and improve the transport of water via such waterways as canals, rivers, and reservoirs.

There are a number of approaches described in traditional hydrological literature that are used to perform flow routing. These approaches can be broadly classified into two categories: (1) hydrodynamic routing methodologies; and (2) hydrological routing methodologies. (Arora et al., 2001). The choice of river routing approaches is a trade off between a number of criterions including the scale of river catchment to be modeled, available data and required accuracy.

The hydrodynamic routing approaches are based on Saint-Venant equations; a continuity equation whichdescribes the balance between input, storage and output in a section of river, and a momentum equation which relates the change in momentum to the applied forces (e.g., Liggett, 1975; Bathurst, 1988; Becker and Serban, 1990). In practice, because Saint-Venant equations are far too complex for normal requirements and require data that are difficult to obtain in large scale basins, hydrological routing models are used more often. (Arora et al., 2001).

The hydrological routing approaches are based on the continuity equation in the Saint-Venant formulation but empirical relationships are used to replace the momentum equation (e.g., Sherman, 1932; Carter and Godfrey, 1960; Cunge, 1969; Dooge et al., 1982; Wilson, 1990) such as the Muskingum, Muskinum-Cunge and the Unit Hydrograph methods. A comprehensive review of hydrological flood routing methods is presented by Weinmann and Laurenson (1979).

A number of routing methodologies are reviewed in this part of the report. These routing methodologies vary from large scale to finer scale routing.

2.1 Hydrological modeling

In general, the hydrological routing applications on large scale routing systems could be listed here:
1- Runoff Routing provides a basis for comparing and validating estimates of streamflow with observed hydrograph data. As most variables describing the state of the surface are not directly observable, river discharge is an appropriate measure to assess model qualities.
2- The simulated fresh water flux into the oceans alters their salinity and may affect the thermohaline circulation (e.g. Wang et al., 1999; Wijffels et al., 1992).
3- Estimates of river discharge from climate change simulations can also be used to assess the impact of climate change on water resources and the hydrology of the major river basins (e.g. Arora et Boer, 2001; Milly et al., 2005; Oki et Kanae, 2006).
4- Influence of river discharge on freshwater ecosystems.

Approaches for routing water through large scale systems are therefore evolving in response to the modeling needs.

In state of the art global routing models, most of the approaches either assume a constant velocity (e.g. Miller et al., 1994; Coe, 1998; Oki et al., 1998) or use simple formulae that use time independent flow velocities parameterized as a function of the topographic gradient (Miller et al., 1994; Hagemann et Dumennil, 1996; Ducharne et al., 2003). These approaches are sufficient to model discharges in monthly or longer time scales. Shorter temporal scales modeling were conducted by using more sophisticated approaches. Notable examples to these approaches were conducted by Arora et Boer (1999), Schulze et al. (2005) who used the Manning's equation to determine time evolving flow velocities as a function of discharge, river cross section and channel slope. In their studies, the Manning roughness coefficient (n) is supposed to be constant globally (Arora et Boer, 1999) or determined by tuning (Schulze et al., 2005). Since values of n vary between 0.015 and 0.07 in natural streams for flows less than bankfull discharge and reach up to 0.25 for overbank flow (Fread, 1993), the assumption of a global constant roughness coefficient or the tuning method contained limitations. These limitations were overcome by the Dingman et Sharma (1997) who developed a relation from objective statistical analysis of over 500 inbank flows.

Latest developments on global routing were achieved by Ngo-Duc, et al. (2007) who developed a variable velocity river routing scheme in the Total Runoff Integrating Pathways model (TRIP). This variable velocity river routing scheme has replaced the constant scheme that was previously developed by Oki et al. (1998).

At the finer regional scale, models have different treatment for surface routing and river routing. In some of these models, two-dimensional routing and/or subsurface water up to a river cell usually precedes one-dimensional routing through a network of river cells. Often, the river network is a set of square cells that is a subset of surface cells.

Amongst finer scale models are CASC2D (Julien, et al., 1995), MODCOU (Ledoux, et al., 1989) and MIKE-SHE (Refsgaard et Storm, 1995). CASC2D is a raster-based model. Within CASC2D, surface routing is done with a 2-dimensional diffusive wave and river network routing with 1-dimensional diffusive in the CASC2D original version (Julien, et al., 1995) and later modified with Preissmann's full dynamic river routing (Ogden, 1994). CASC2D has been lately applied to the Quabrado Estero watershed in Costa Rica (Marsik et al., 2006). Downer et al. (2002) offer a comprehensive discussion of the evolution of CASC2D with a review of its previous applications.

MIKE-SHE (Refsgaard and Storm, 1995) is based on the SHE (Système Hydrologique Européen; Abbott et al., 1986) model. It is a fully distributed and physically based modeling system. A finite difference approach is used to solve the partial differential equations describing the processes of overland (two-dimensional Saint-Venant equation), channel (one-dimensional Saint Venant equation). An application of the MIKE-SHE model could be found in the study conducted by Sahoo, et al. (2006) who used Manning's equation with different Manning's coefficients for surface and river routing.

Other routing approaches include the association between hydrological and hydraulic models, such as the coupling between the MIKE-SHE and MIKE-11 hydraulic model (Thompson et al., 2004) and the HEC-HMS/HEC-RAS (Kneble, et al., 2005). In the MIKE-SHE/MIKE-11 (Thompson et al., 2004) study the connection between surface cells and river reach is done on a nearest-neighbor basis. While in the HEC-HMS/RAS studies (Knebl, et al., 2005) watershed routing was performed up to river gages with HEC-HMS and then routing within a river reach is performed by HEC-RAS.

2.2 Simplified hydraulic modeling

Complex hydraulic models such as HEC-RAS, MIKE-11 use the Saint Venant equations, and therefore rely on many high resolution morphological parameters (cross sections). These morphological parameters are often unknown at larger scales. Estimation of these parameters through optimization is cost prohibitive.

Large scale hydraulic routing techniques are usually based on the conversation of mass and a simplified form of the conservation of momentum equation. A number of these techniques are hereby reviewed.

2.2.1 *Manning's equation*

Some routing models use the general form of Manning's equation to relate stream flow as a function of depth for all reaches in a segment (Chow et al, 1988, P.159):

$$Q = \frac{1}{n} A R^{2/3} S_o^{1/2} \qquad (1)$$

where:

A is the area of flow
n is Manning's roughness coefficient (dimensionless)
R is the hydraulic radius of the stream
S_o is the slope of the channel in the longitudinal profile (dimensionless)

The wetted perimeter and hydraulic radius of a stream, which are needed in Manning's equation, are often complicated functions of depth, and can only be solved analytically by making assumptions to simplify the channel geometry. One of the approaches was assuming a wide rectangular channel (Shen and Julien, 1993). This assumption approximates the wetted parameter as equal to the stream width and results in approximation of the hydraulic radius that is equal to stream depth. Solving the equation of Manning for stream depth then yields (Prudic et al, 2004)

$$D = \left[\frac{Q * n}{w s_o^{1/2}} \right]^{3/5} \qquad (2)$$

where:

w is the stream width
D is the depth of the water

2.2.2 *Kinematic-wave equation*

The kinematic-wave equation is a simplified approximation of the Saint Venant equations. It approximates the Saint-Venant equations for computing flow through rectangular or non-prismatic channels. The kinematic-wave equation for routing flow in streams can be written (Lingthill et Whitham, 1955):

$$\frac{\partial Q}{\partial x} + \frac{\partial A}{\partial t} = q_l \qquad (3)$$

where:

A is the wetted cross sectional area (L^2)
Q is the discharge (L^3/T)

Several forms of the momentum equation are combined with equation (3) to route flow to downstream channels. The form of the momentum equation differs in how the channel cross-sectional dimensions and channel slopes are represented in Manning's equation.

The kinematic-wave approximation neglects the dynamic component of flow that is represented by the derivative terms in the more complete form of the momentum equation in the Saint-Venant equations. It assumes that gravitational forces are balanced by frictional forces such that:

$$S_o = S_f \qquad (4)$$

where:

S_o is the slope of the channel in the longitudinal profile (dimensionless)
S_f is the friction slope of the channel in the longitudinal profile (dimensionless)

Another approach represents momentum by using tables of specified values from stream flow gages, or the power-law equations described by Prudic et al. (2004, P.6-9). Momentum caused by the water-surface slope, velocity head, and acceleration is neglected.

2.2.3 Diffusion wave equation

Another less simplified approximation of the Saint-Venant equations combines the spatial derivative from the momentum equation with the continuity equation, which results in a second derivative term in the continuity equation (Lighthill etWhitham, 1955). The second derivative term in the continuity equation causes the flood wave to spread upstream slightly and is commonly referred to as a diffusion analogy for the dynamic component of the momentum equation. This approach is the basis for the surface-water flow model called DAFLOW (Jobson et Harbaugh, 1999) that was coupled with MODFLOW.

The simplified form of the momentum equation is:

$$s_f - \frac{\partial h}{\partial x} = 0 \qquad (5)$$

Equation (5) allows for upstream directed flows. Brakensiek (1965) solved the equations with a four point centered implicit finite difference solution techniques. Harder and Armacost (1966) used an explicit finite difference solution technique. The nonlinear diffusion wave model is a significant improvement over the kinematic model because of the inclusion in eq.5 of the water surface face slope term ($\partial h/\partial x$). This term allows the diffusion model to describe the attenuation (diffusion effect) of the flood downstream extremity of the reach to account for backwater effects. It does not use the inertial terms of the momentum equation, therefore, is limited to slow moderately rising flood waves in channels of rather uniform geometry.

2.3 Empirical models

2.3.1 Lag models

Some flood routing models are based on the intuition and observations of past flood wave motion. One category of empirical models is the lag models, in which lag is the time difference between inflow and outflow within a routing reach. The successive average-lag method developed by Tatum (1940) assumes that there is some point downstream where the (I_2) at time (t_2) is equal to an average flow, i.e., $(I_1+I_2)/2$. Tatum found that the number of successive averages occurring within a reach was approximately the time of travel of the wave divided by the reach length. Outflow at the end of the reach is computed by:

$$O_{n+1} = C_1 I_1 + C_2 I_2 + \cdots\cdots C_{n+1} I_{n+1} \qquad (6)$$

where n is the number of sub-reaches (successive averages) within the routing reach. The routing coefficients used in the method can be obtained via the Tatum’s approach or by trial and error using observed inflow and outflow hydrographs.

2.3.2 Power law equations

Another method to compute water depths in streams is by using power law equations for a stream segment that relate stream depth and width to stream flow using the following two equations (Leopold et al., 1953)

$$D = cQ^m \text{, and } w = aQ^b \qquad (7)$$

where:
w is the stream width *(L)*
*D*is the stream depth *(L)*
c and *a* are empirical coefficients determined from regression methods
m and *b* are empirical exponents determined from regression methods (dimensionless)

The regressions typically are determined at streamflow gauging stations. Representative values of the numerical coefficients for selected regions of the United States are listed in Leopold et al. (1992, table 7-5).

2.3.3 Gage relations

Other empirical techniques include gage relations (Linsley et al., 1949) which relate the flow at a downstream point to that at an upstream station. Gage relations can be based on flow, stages or a combination of each. The effect of lateral inflow is automatically contained in the empirical relation.

Empirical relations are limited to the applications with sufficient observations of inflows and outflows to calibrate the essential coefficients. They provide best results when applied to slowly fluctuating rivers with negligible lateral inflows and backwater effects. They are extremely economical in computational requirements; however, considerable effort me be required to derive the empirical coefficients.

3 Modeling methodology

The modeling methodology in this study is based on the association between a hydraulic and a hydrological model. The production of lateral inflows draining in the river reach is simulated by the hydrogeological model MODCOU (Ledoux, 1980; Ledoux et al., 1984, 1989) while the routing within the river reach is performed by hydraulic model HEC-RAS (US Army Corps of Engineers, 2002).

3.1 Hydrological modeling using the MODCOU model

The introduction of physically-based distributed modeling of catchment hydrodynamics, by Freeze and Harlan in 1969 and followed by other models such as the SHE model (Abbott et al., 1986) and MODCOU (Ledoux, 1980; Ledoux et al., 1984, 1989) has marked a shift towards such physically-based models. Meantime introduction of geographical information systems and increased computer power has favored the use of such models.

At present a great variety of systems are being used regularly for both research and practical applications, ranging from fully physically-based distributed systems such as MODCOU (Ledoux et al., 1989) and MIKE SHE (Refsgaard et al., 1995) towards semi-distributed conceptual systems such as WATBAL (Knudsen et al., 1986) and TOPMODEL (Beven et Kirkby, 1979).

MODCOU is a regional spatially distributed model, which describes surface and groundwater flow at a daily time step. It uses a conceptual reservoir-based approach in every cell of the surface layer to partition precipitation into evapo-transpiration, surface runoff (resulting from overland flow and interflow) and infiltration. The structure of the coupled model is illustrated in figure 1.

MODCOU calculates the daily water balance in the hydrological system, the flow in rivers and the piezometric variations in aquifers, using standard climatic data (rainfall, PET).

Infiltration recharges the groundwater that can consist of a single or multi-layered aquifer. A delay is imposed between surface infiltration and aquifer recharge using a cascade of equal linear reservoirs through the unsaturated zone (Nash and Sutcliffe, 1970). The recharge flow contributes to the dynamics of groundwater, given in each aquifer layer by a finite-difference solution of the two-dimensional diffusivity equation.

The resulting groundwater head is dynamically coupled to the water level in surface “river” cells. This defines the base flow component of river-flow which also includes surface runoff and is routed through the drainage network with transfer times that depend on topography and a basin-wide parameter, the concentration time.

The superficial in MODCOU is discretized by a progressive multi-scale grid of embedded square meshes, the size of each cell is typically varying from 1to 8km. The groundwater domain is modeled by a progressive multi-scale grid with a multi-layer structure.

MODCOU has successfully predicted surface and groundwater flow in many French basins of varying scales and hydrogeological setting. Among application examples of MODCOU: Haute-Lys and Caramy basins (Ledoux, 1980); HAPEX-MOBILHY study (Boukerma, 1987); the Fecht river basin (Ambroise et al., 1995); the Rhône basin (Golaz, 1999; Habets et al., 1999; Etchevers et al., 2002), the Seine basin (Gomez et al., 2001) and the Somme basin Habets et al., 2009).

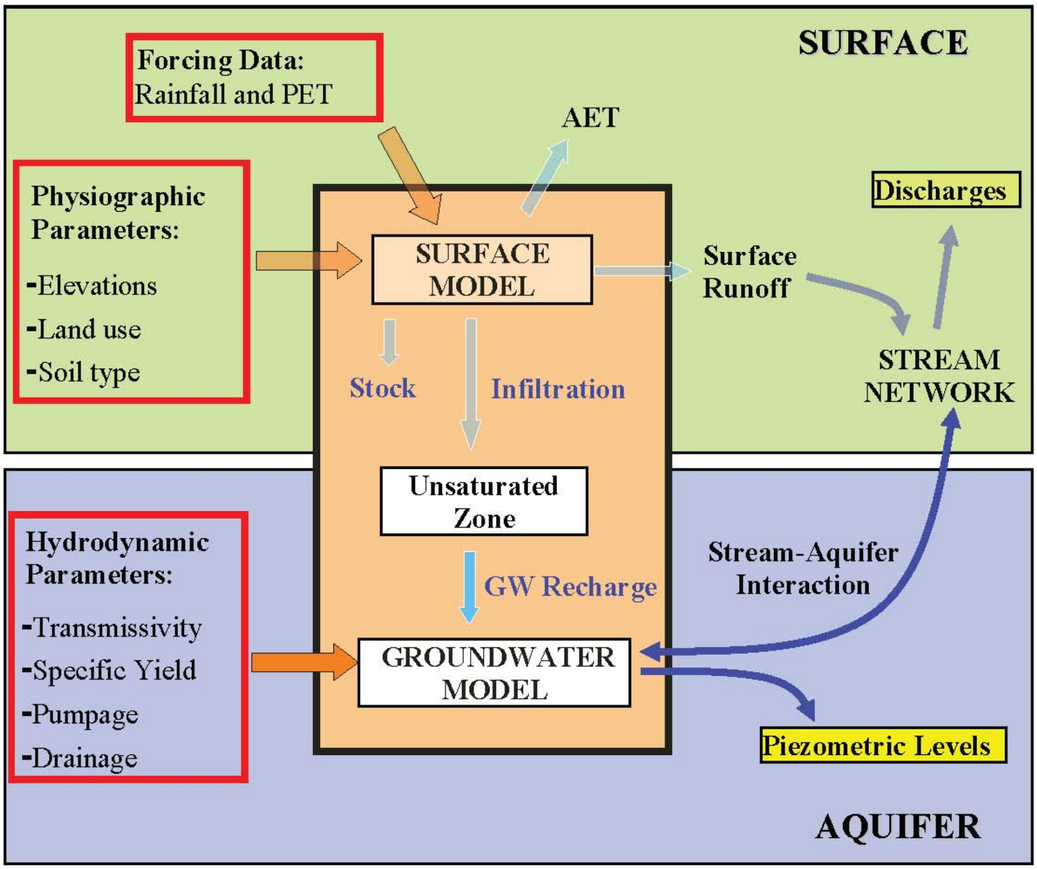

Fig. 1 Structure of MODCOU model

The stream routing methodology in MODCOU is based on the derivations of the model CEQUEAU (Girard et al. 1972). The stream network is divided into segments by using isochrones (figure 2).

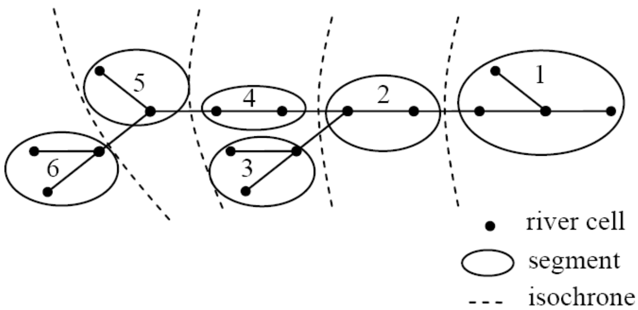

Fig.2 Formation of segments on the stream network.

Each segment represents a group of river cells between two isochrones and has a drainage coefficient. The segments are formed in such a way that water in each cell inside a segment arrives at the outlet of the basin within the same time step. Therefore, the surface water stock contained in a segment in a given time step is the sum of the water stock in all the river cells forming that segment.

The transfer is carried out as follows:

$$Vs_i^{t+1} = (1 - Cds_i)\cdot(Vs_i^t + Qr_i^t + Qaq_i^t) + \sum_{j=1}^{Nup} Cds \cdot (Vs_j^t + Qr_j^t + Qaq_j^t) \quad (8)$$

where Vs_i^{t+1} is the volume of water in segment i at time $t+1$; Cds_i is the discharge coefficient of segment i;

Nup is the number of upstream segments which flow directly into segment *i* (e.g. segments 3 and 4 for segment 2 as in figure 2 ; Qr_i is the total volume of surface runoff flowing into segment *i* within the time step; Qaq_i is the total volume of water exchanged with the aquifer in segment *i* within the time step. For any given segment, *Qr* and *Qaq* are computed with the following equations:

$$Qr^t = \sum_{i=1}^{n_r} qr_i^t \quad (9)$$

where qr_i is the volume of surface runoff arriving at the river cell *i*, and n_r is the number of river cells in the segment.

$$Qaq^t = \sum_{t=1}^{n_r} qaq_i^t \quad (10)$$

where: *qaq* is the volume of water exchanged between a river cell and the aquifer cell beneath in a time step.

Eq. 10 is considered to be the equation of continuity for a segment, which means that the volume of water in a segment is equal to the volume of water retained after discharge and plus, the discharged volumes coming from upstream segments.

The stream flow may be simulated at any point on the stream network in order to output the flow hydrograph and compare it with the measured stream flow data.

Once the transfer between the segments is completed, the total amount of water in a segment is distributed among the river cells by using a redistribution coefficient:

$$Cred_i = \frac{l_i / Cd_i}{\sum_{k=1}^{n_r} l_k / Cd_k} \quad (11)$$

where: n_r is the number of river cells in the segment, *l* is the size of the cell, and *Cd* is the discharge coefficient of the cell.

The redistribution of the volume of water for a cell is made using the following:

$$V_i^{t+1} = Cred_i \cdot Vs^{t+1} \quad (12)$$

3.2 Hydraulic modeling using HEC-RAS

Hydraulic modeling of natural rivers could be successfully analyzed with four equations: continuity, energy, momentum, and Manning. The Manning equation is considered to be empirical and is used to estimate friction loss while the energy equation is considered semi-empirical. (Dyhouse et al., 2003).

One-dimensional (1D) flow routing approaches such as Mike-11 (DHI, 1995), ISIS (HR Wallingford, 1997), FLDWAV (Fread et al., 1998) and HEC-RAS (USACE, 2002), based on the Saint Venant Equations or variations, still form the majority of traditional numerical hydraulic models used in practical river engineering. The widespread usage in practice might be explained not only by the fact that 1D models are (in comparison to higher dimensional hydraulic models) simpler to use and require a minimal amount of input data and computer power, but also because the basic concepts and programs have already been around for several decades (Stoker, 1957; US Army Corps of Hydraulic Engineers, 2001; Pappenberger, 2005).

In this study, the hydraulic model used is HEC-RAS. HEC-RAS is a public domain model developed by the US Army Corp of Engineers (USACE, 2002). It performs one dimensional steady and unsteady flow calculations on a network of natural or man-made open channels.

Basic input data required by the model include the channel network connectivity, cross-section geometry, reach lengths, energy loss coefficients, stream junctions information and hydraulic structures data. Cross - sections are required at representative locations throughout a stream reach and at locations where changes in discharge, slope, shape or roughness occur. Boundary conditions are necessary to define the starting water depth at the stream system endpoints, i.e., upstream and downstream. Water surface profile computations begin upstream for subcritical flow or downstream for supercritical flow. Discharge information is required at each cross-section in order to compute the water surface profile. HEC-RAS solves the mass and momentum equations (eq.12 and eq.13) using implicit finite difference approximations and Preissman's second-order scheme. The computation engine for the HECRAS 1-D unsteady flow simulator is based on the USACE's UNET model (Barkau, 1985; USACE, 2002).

$$\frac{\partial Q}{\partial x}+\frac{\partial A}{\partial t}-q_l=0 \tag{12}$$

where: Q = Discharge (L^3/T)
A = Cross Sectional Area (L^2)
x = The distance along the longitudinal axes of the channel or floodplain (L)
t = Time (T)
q_l = Lateral inflow per unit length ($(L^3/T)/L$)

$$S_f = S_0-\frac{\partial y}{\partial x}-\frac{V}{g}\frac{\partial V}{\partial x}-\frac{1}{g}\frac{\partial V}{\partial t} \tag{13}$$

a ***b*** ***c*** ***d*** ***e***

where: S_o = Bottom slope
S_f = Friction slope
V = Velocity (L/T)
y = Flow depth (L)
g = Acceleration due to gravity (L/T^2)

Term ***a*** is the friction slope and reflects the resistance to flow. Term ***b*** is the bed slope and reflects the body force from gravity. Term ***c*** is the pressure term and reflects the change in depth in the longitudinal direction. Term ***d*** is the convective acceleration and reflects both spatial variation of the flow ($\partial Q/\partial x$) and longitudinal change in the cross-section area ($\partial A/\partial x$). Term ***e*** is the local acceleration and reflects unsteady flow. Terms ***b*** and ***c*** combine to give the water-surface slope.

Figure 3 illustrates the two-dimensional characteristics of the interaction between the channel and floodplain flows. When the river is rising water moves laterally away from the channel, inundating the floodplain and filling available storage areas. As the depth increases, the floodplain begins to convey water downstream, generally along a shorter path that of the main channel, and when the river stage is falling, water moves toward the channel from the overbank supplementing the flow in the main channel.

Because the primary direction of flow is oriented along the channel, this two-dimensional flow field can often be accurately approximated by a one-dimensional representation. Off channels ponding areas can be modeled with storage areas that exchange water with the channel. Flow in the overbank can be approximated as flow through a separate channel (USACE, 2002).

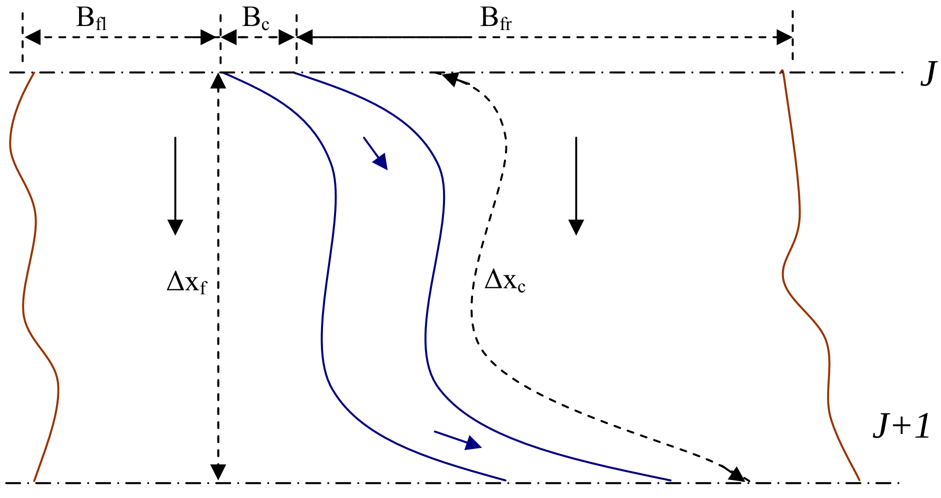

Fig.3 Two-dimensional characteristics of the interaction between the channel and floodplain flows (USACE, 2002)

Channel and floodplains problems have been addressed in many different ways. A common approach is to ignore overbank conveyance entirely, assuming that the overbank is used only for storage. This assumption may be suitable for large streams such as the Mississippi River where the channel is confined by levees and the remaining floodplain is either heavily vegetated or an off-channel storage area. Fread (1976) and Smith (1978) approached this problem by dividing the system into two separate channels and writing continuity and momentum equations for each channel. To simplify the problem they assumed: (1) a horizontal water surface at each cross section normal to the direction of flow, (2) the exchange of momentum between the channel and the floodplain was negligible, (3) the discharge was distributed according to conveyance, i.e.:

$$Q_c = \phi Q \tag{14}$$

where:

$$\phi = \frac{K_c}{K_c + K_f} \tag{15}$$

$$K = \frac{1}{n} A R^{2/3} \tag{16}$$

$$Q = K S^{1/2} \tag{17}$$

where: ϕ = Discharge distribution factor (dimensionless)

Q_c = Flow in channel (L^3/T)
Q = Total flow (L^3/T)
K_c = conveyance in the channel (a measure of the carrying capacity of a channel)
K_f = conveyance in the floodplain
n = Manning's roughness coefficient (dimensionless)
A = Flow area (L^2)
R = Hydraulic radius (L)

With the above three assumptions, the one-dimensional equations of motion can be combined into a single set:

$$\frac{\partial A}{\partial t} + \frac{\partial(\phi Q)}{\partial x_c} + \frac{\partial[(1-\phi)Q]}{\partial x_f} = 0 \tag{18}$$

$$\frac{\partial Q}{\partial t} + \frac{\partial(\phi^2 Q^2 / A_c)}{\partial x_c} + \frac{\partial((1-\phi)^2 Q^2 / A_f)}{\partial x_f} + g A_c \left[\frac{\partial y}{\partial x_c} + S_{fc}\right] + g A_f \left[\frac{\partial y}{\partial x_f} + S_{ff}\right] = 0 \tag{19}$$

in which the subscripts c and f refer to the channel and floodplain, respectively. In HEC-RAS these equations are approximated using implicit finite differences, and the full nonlinear equations solved numerically using the Newton-Raphson iteration technique. The model was successful and produced the desired effects in test problems.

Expanding the earlier work of Fread and Smith, Barkau (1982) manipulated the finite difference equations for the channel and floodplain and defined a new set of equations that were computationally more convenient. Using a velocity distribution factor, he combined the convective terms. Further, by defining an equivalent flow path, he replaced the friction slope terms with an equivalent force.

The equations derived by Barkau are the basis of UNET which was then Integrated in HEC-RAS as the unsteady flow simulator routine. The full equations and their derivations could be found in UNET Users Manual (Barkau, 2001)

A full description of the model and its computational schemes is given in the USACE HEC-RAS website www.hec.usace.army.mil.

3.3 Summary of differences between the MODCOU and HEC-RAS routing techniques

The major differences difference between the hydrological routing in MODCOU and the hydraulic routing in HEC-RAS are illustrates in table 1.

Table 1. Major differences difference between the MODCOU routing and HEC-RAS routing

Comparison	MODCOU hydrological routing	HEC-RAS hydraulic routing
Type of routing	Hydrological routing	Hydraulic routing
Routing technique	Conservation of mass and empirical storage-flow relations to approximate momentum effects	Saint Venant equations (continuity and momentum equations)
Input Data	Very economic from the data perspective as it only require stream flow hydrographs as input data	Require high resolution physical data describing the channel geometry, gradient and flow resistance characteristics
Hydraulic structures	Not taken into consideration	All hydraulic structures are considered
Δt (computational time step)	≥ 1 day	≥ 1 second
Δx (computational distance step)	River cells of 1 km	Distance between cross sections (no limit)
Applications	Could not be applied to flow problems with sudden dynamic change such as dam break problems	Could be applied to dynamic problems, such as dam breaches or ice jam release events
Basin scale	Large basin scale applications (e.g. Seine River basin)	Finer basin scale applications (e.g. San Antonio River basin)
Simulated variables	Discharge hydrographs at river cells and gauging stations	Ability to produce output describing both water levels and discharge hydrographs at cross sections and gauging stations
Interactions with ground water	Interaction with groundwater cells	Coupling is possible with MODFLOW

4 Area of study (Serein River):

The Serein River is a sub tributary of the Seine River, with a length of 186 km. The source of the Serein is at Saulieu (close to Morvan), and it meets the right bank of the Yonne at Bassou. Figure 4 illustrates the Serein's location within the basin of the Seine.

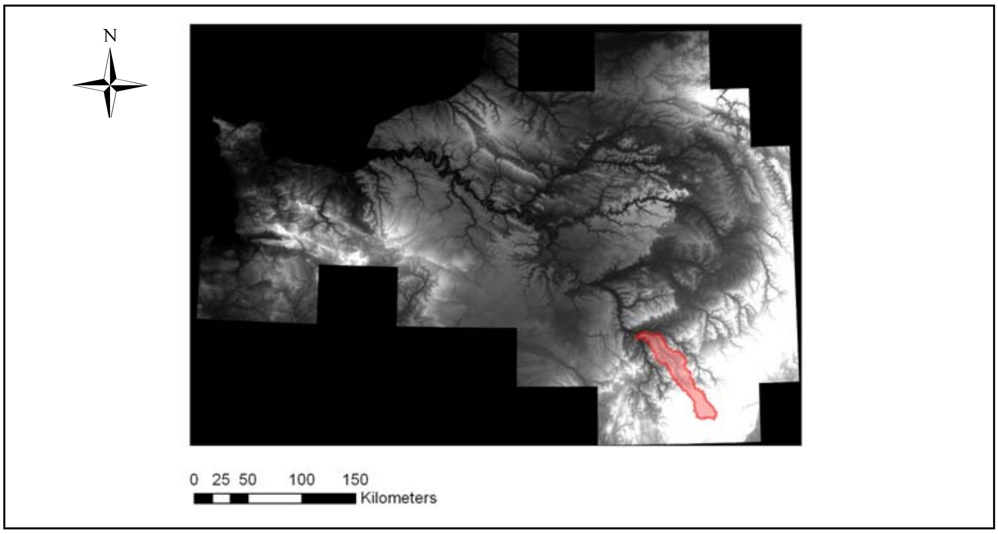

Fig.4 The location of the Serein River within the basin of the Seine

The Serein River has a simple hydrographic network with no major tributaries. Additionally, no hydraulic structures are located within the studied reach which makes it is less complicated to count for potential loss in energy grade line and water volume. The necessary data to construct the hydraulic model are well documented in the Serein River. The river geometrical profiles of the river are surveyed by the Direction Régionale de l'Environnement (DIREN). The availability of well documented data allows maximum number of sensitivity analysis with fewer uncertainties, hence allowing us to identify the importance of each hydraulic factor or boundary condition composing the hydraulic model, and further more identifying the influence of boundary conditions and geometry when simplified or degraded.

In terms of flooding, The Serein River has witnessed important flooding events during the last two centuries, such as the floods of May 1836, May1856, September 1866, 21 January 1910, 28 April 1998 and March 2001

Within the considered study reach, the Serein runs about 87 km starting from Dissangis and ending at Beaumont (just before the confluence with the Yonne River). The control point where calibration was held is located at Chablis (55 km from Dissangis). The selection of this reach was based on the availability of unsteady flow simulation and geometrical data. Figure 5 illustrates the Serein River and its sub-catchments within the studied area.

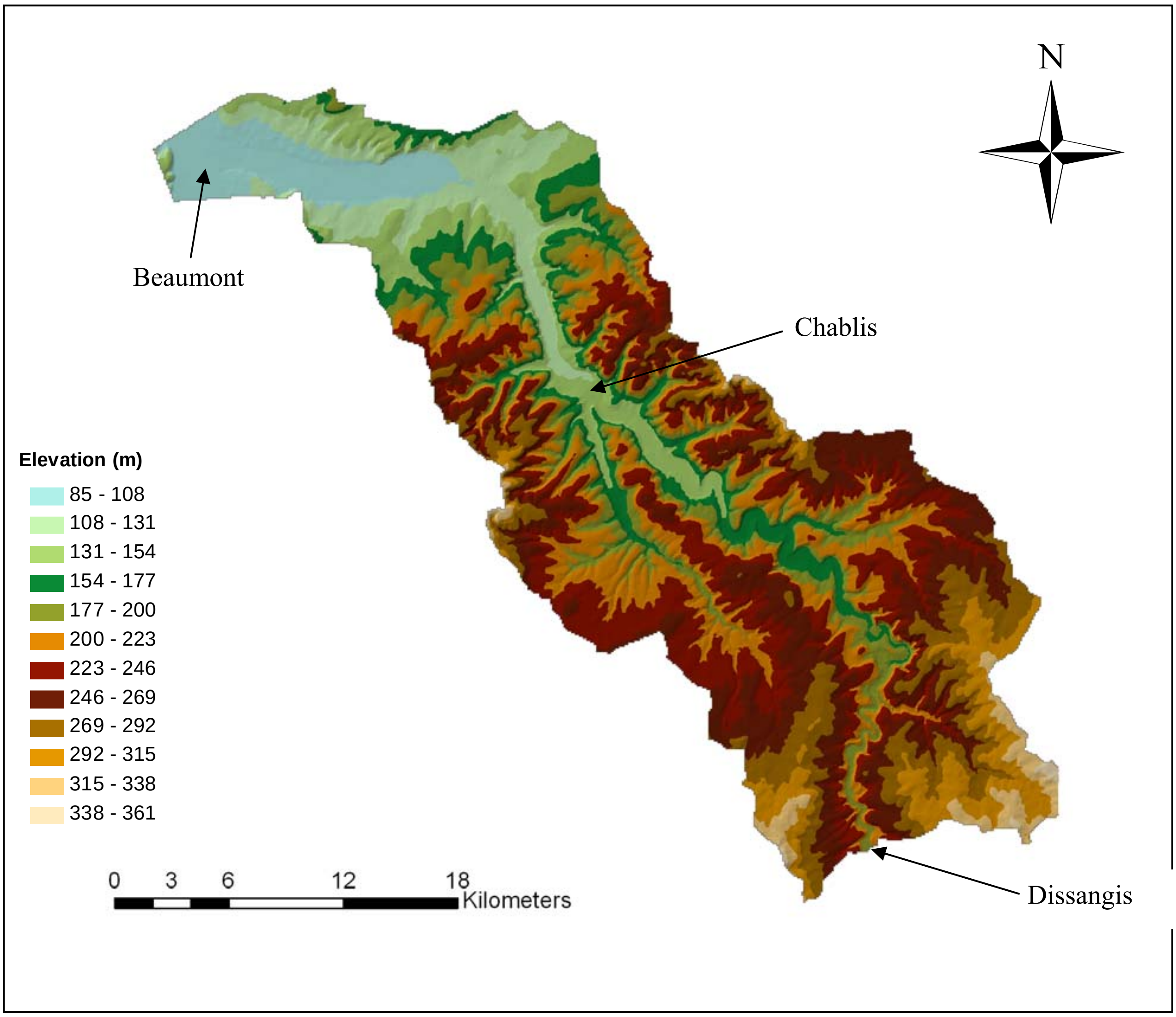

Fig.5 The Serein River between Dissangis and Beaumont

The Serein River presents an important seasonal discharge fluctuation. High flows occur in winter and spring, with an average monthly rates ranging between 12.4 and 17.5 m3/s, while a gradual decline is noticed in summer (July-September) with flow dropping to1.14 m3/s in August.

Observed discharge and water levels in the three major hydrometric stations (Dissangis, Chablis, and Beaumont) are available for the use in boundary conditions and calibration. The observed average discharge at major hydrometric stations of the Serein River are illustrated in table 2.

Table 2. The observed discharge at the main stations along the Serein River

Station Code	**Location**	**Period**	**Average Discharge m^3/s**	**Catchment Area km^2**
H2332020	Dissangis	1/Aug/1997 – 31/Jul/2005	4.72	643
H2342010	Chablis	1/Aug/1997 – 31/Jul/2005	8.6	1120
H2342030	Beaumont	6/Nov/1997 – 31/Jul/2005	11.43	1337

Figure 5 illustrates the observed mean annual discharge of the Serein River in the three major hydrometric stations of the Serein River. The figure illustrates the practicality of the hydrological year 2001 which witnessed on of the major flooding of the Serein River.

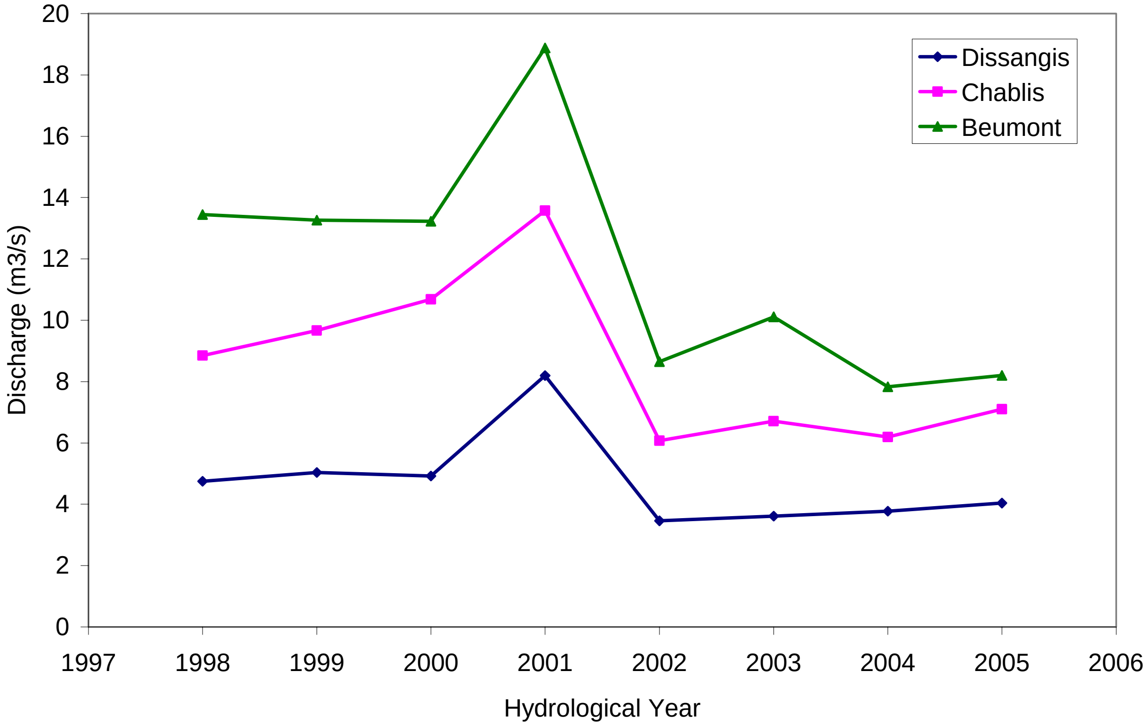

Fig 6. Mean annual discharge in the three major hydrometric stations of the Serein River

5 The construction of the Serein River model

Successful hydraulic simulation depends to a great point on the availability of accurate data such as river cross sections geometry and observed stage and discharge hydrographs in river reaches. Figure 7 illustrates the required input data in general to construct a hydraulic or flood routing model.

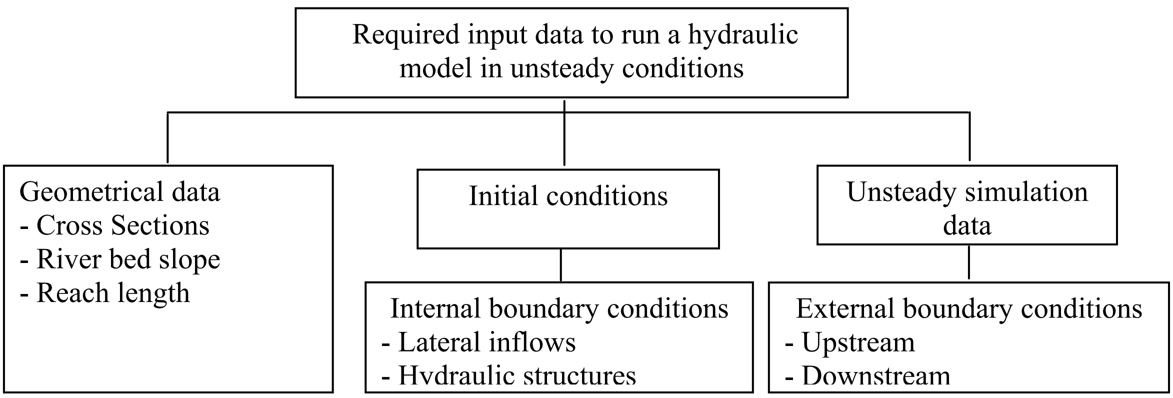

Fig.7 Required input data to construct a hydraulic model

The input data used to construct the Serein River model is summarized in table 3. No hydraulic structures along the studied reach exist (as stressed previously). The presence of bridges along the river reach was neglected from the geometry representation of the model.

Table 3. Serein model input data

River Geometry	Upstream boundary condition	Downstream Boundary condition	Lateral inflow
20 surveyed cross sections	Observed discharge hydrograph	Rating curve at Dissangis	Simulated by MODCOU

The Geometry data is represented by 20 surveyed cross sections containing the main channel and floodplains. The sections were surveyed by the Direction Régionale de l'Environnement (DIREN) in 2007. The distances between surveyed cross sections vary from 2 km to 10 km, this variation depends on where water surface elevations are required, sudden changes in river cross sectional properties and difficulties faced on the ground while surveying the river. The widths of floodplains vary from 100 to 600 meters according to the topographical characteristics of the area and the meanders along the river.

Each cross section is defined by a set of points surveyed perpendicularly to the main stream of the river and its floodplains, each point has an X, Y, and Z Lambert II system coordinates, where Z is the elevation (in meters) above a datum.

The upstream boundary condition of the Serein model is defined by a observed mean daily discharge hydrograph at Dissangis (figure 8). The period of the input discharge hydrograph is from 1 August 1997 to 31 July 2005. The observed discharge hydrograph shows the two important flood events (April 1998 and March 2001) that occurred within the period of simulation.

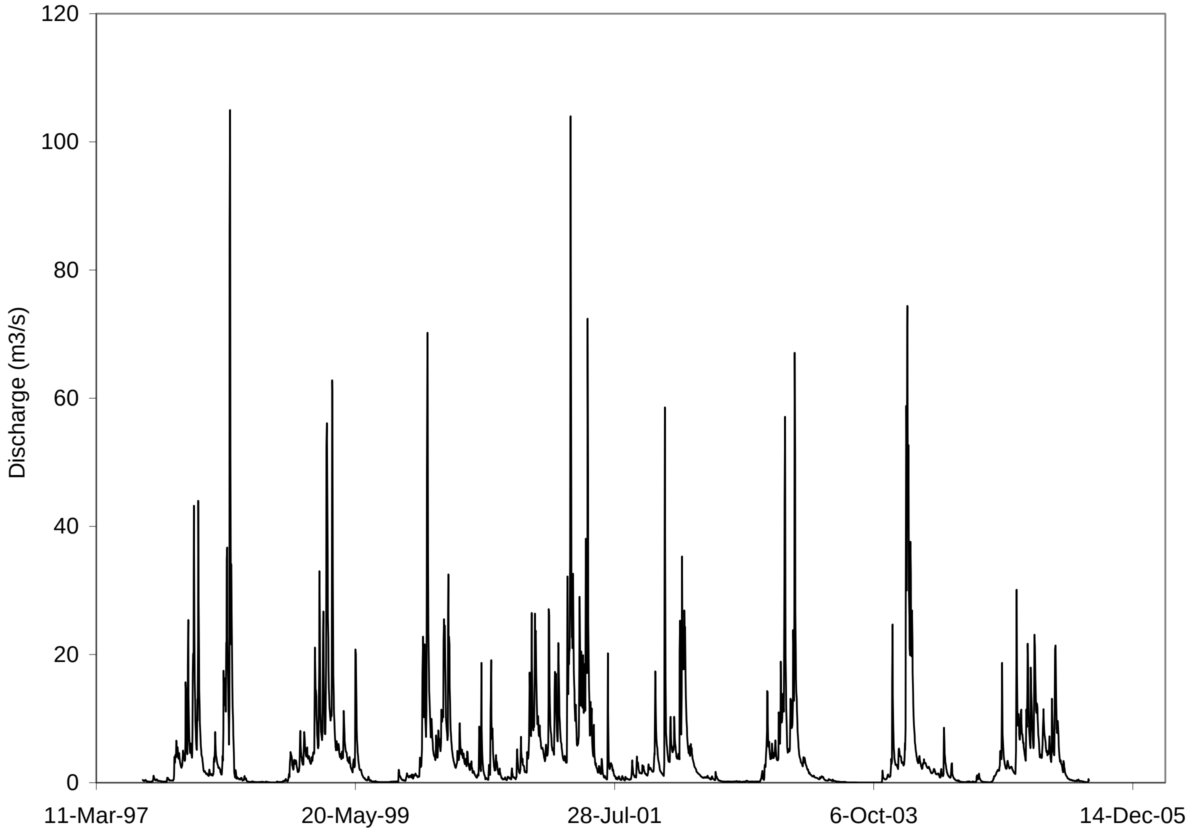

Fig.8 Observed Discharge hydrograph at Dissangis from 1/Aug/ 1997 to 31/Jul/2005

The downstream boundary condition of the Serein River model is a single valued rating curve (monotonic function of stage and flow) at Beaumont (Figure 9).

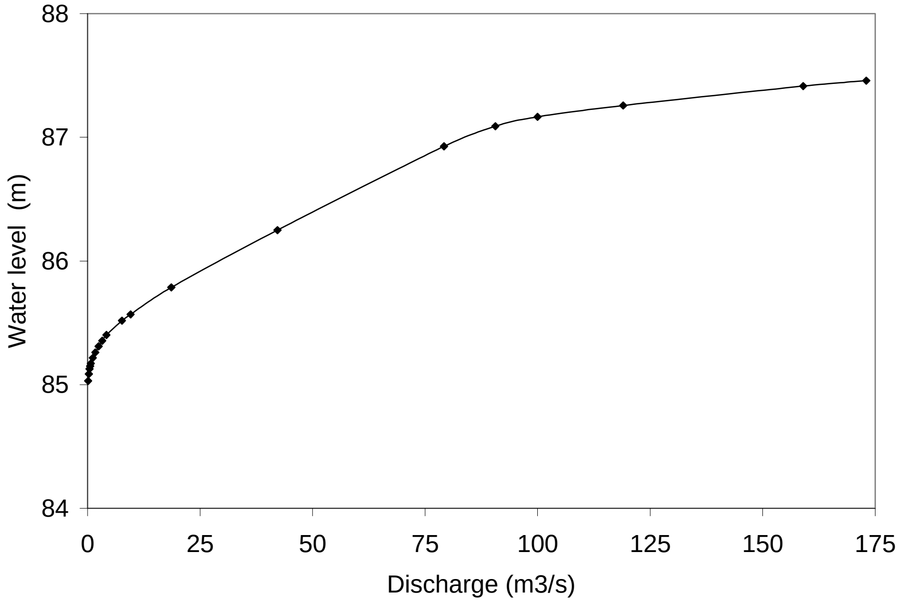

Fig.9 Observed rating curve at Beaumont

The total area draining in the river reach between Dissangis and Beaumont is 694 km^2 , which represents a catchment area even larger than the upstream catchment area of Dissangis (643 km^2). It is obvious that lateral inflows have an important and non negligible role in the Serein River. These lateral inflows draining into the river reach are simulated by the hydrological model MODCOU. The model MODCOU represents the river lateral inflows by a mesh composed of square cells of 1*1 km area. Each river cell of MODCOU produces a daily volume of water. Figure 10 illustrates the sub basins of the Serein River between Dissangis and Beaumont with MODCOU river cells representing the river. The studied reach between Dissangis and Beaumont is represented by 76 MODCOU river cells.

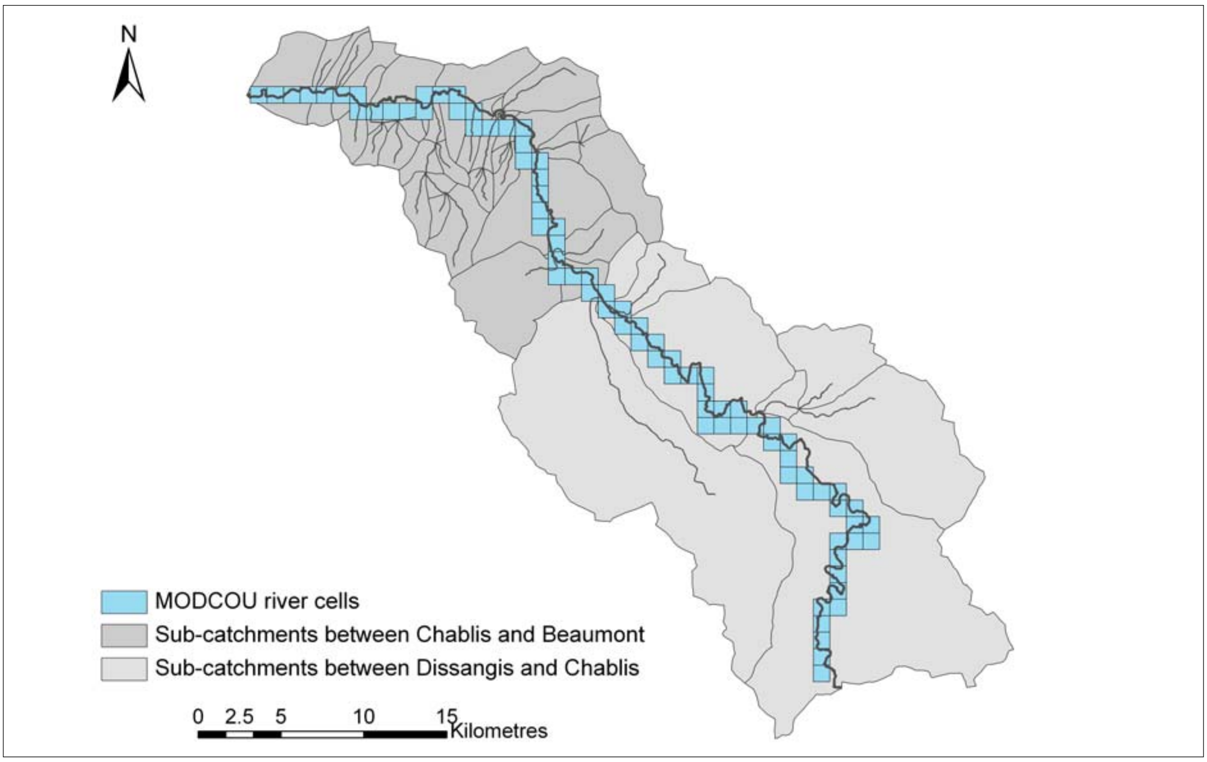

Fig. 10 Sub-catchments and MODCOU river cells of the Serein River between Dissangis and Beaumont

An example of lateral inflow produced by one river cell of MODCOU is illustrated in figure 11.

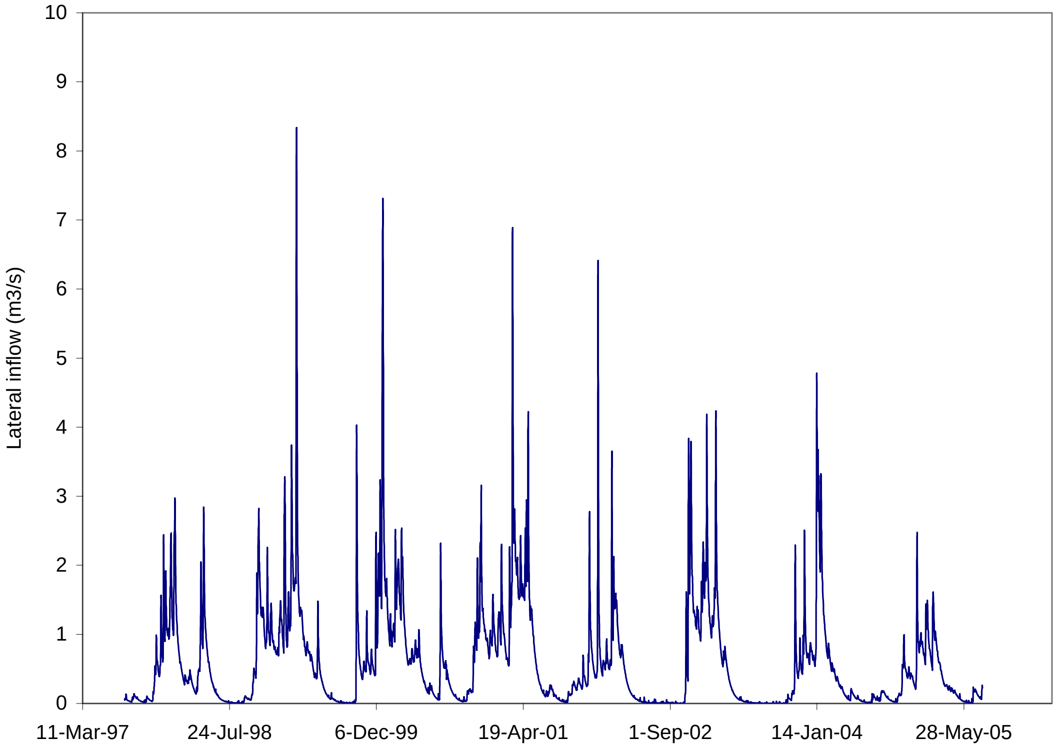

Fig. 11 Example of a lateral inflow produced by one river cell of MODCOU

To spatially project the MODCOU river cells discharge along the Serein River reach, a linear relationship between the river cells of MODCOU and the Serein River reach is developed (figure 12). The discharge produced by each river cell is uniformly distributed over 1.3 km of the Serein River reach.

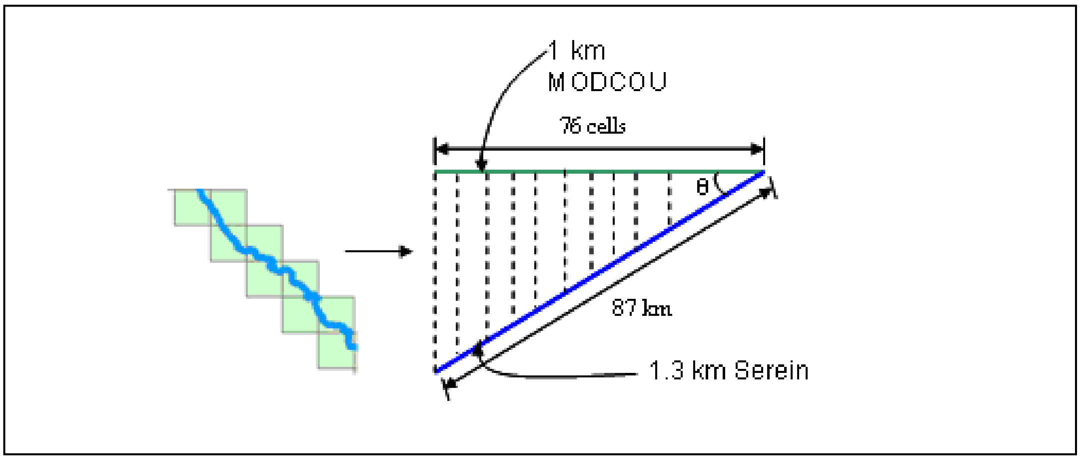

Fig. 12 Spatial projection of MODCOU river cells discharge over the Serein River reach

5.1 Selection of the model's temporal and spatial Computational factors

An important step in unsteady flow simulation models based on the one-dimensional Saint-Venant equations is the proper selection of computational parameters represented in time and spatial intervals. These parameters influence the accuracy, convergence, robustness and stability of the numerical model (Fread et al., 1993).

If the selected values (Δt , Δx) are too small, the computations are inefficient sometimes to the extent of making the application too expensive or time consuming and therefore time infeasible. If these values are too large, the resulting truncation error (the difference between the true solution of the partial differential Saint-Venant equations and the approximate solution of the four-point implicit finite difference approximations) can cause significant errors in the computed discharges and corresponding water surface elevations; the errors may be so large as to make the computations totally unrealistic. Unrealistic solutions can cause computer program to abort when computed elevation result in negative depths; also, unrealistic solutions can result in significant irregularities (spurious spikes) in the computed hydrographs.

5.1.1 Temporal computational factor (Δt)

Through several years of experience with dynamic routing models in numerous applications and by using numerical convergence testing for a wide spectrum of unsteady flow applications, Fread (1993) developed an empirical selection criterion between the time step and the hydrograph time of rise:

$$\Delta t \approx \frac{T_r}{20} \tag{20}$$

Where T_r is the hydrographs time of rise (time from the significant beginning of increased discharge to the peak of the discharge hydrograph), in hours.

Figures 13 and 14 respectively illustrate the observed rising time of the two major peaks (April 1998 & March 2001) at Dissangis. The peak of April 1998 has a rising time of 19 hrs while the peak of March 2001 has a rising time of 21 hrs. According to eq.20 the computational time step is ~1hr.

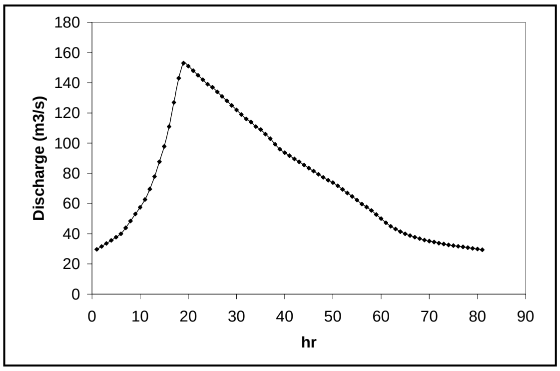

Fig.13 Hourly readings at Dissangis from 27/Apr/98 00:00 to 30/Apr/98 8:00

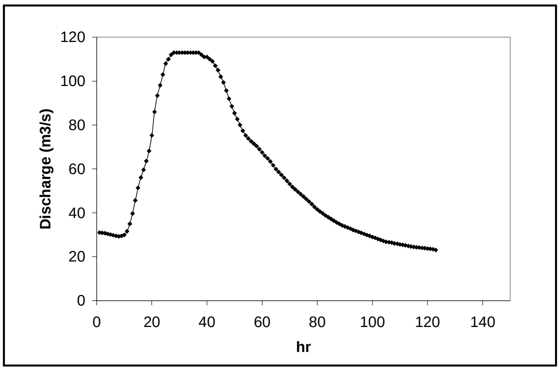

Fig.14 Hourly readings at Dissangis from 13/Mar/01 8:00 to 18/Mar/01 8:00

Other time step increments were also tested (0.5, 3, 4, 6, 12, 18, 24 hrs). The comparison between the different time steps showed that produced water level and discharge hydrographs are not sensitive to the variation of Δt from 0.5 to 3 hours. It should be stressed that the variation of Δt from 0.5 to 3 hrs influenced the time of simulation, as larger time steps required more time to complete the simulation. When using a Δt larger than 4 hrs, a slight numerical oscillation occurs. Increasing the time steps to 6, 8, 12, 18 and 24 hrs caused larger numerical oscillations and hence failure in the matrix solution.

5.1.2 Spatial computational factor (Δx)

Cross sections should be placed at representative locations to describe the changes in geometry, discharge, slope, velocity, and roughness. Cross sections must also be added at levees, bridges, culverts, and other structures.

There is no hard and fast guidance concerning the appropriate distance between cross sections. In the author's experience, large rivers (rivers with several thousand square miles of watershed) on low slopes (less than1 m/km) can have a maximum cross-section spacing of approximately 750 m. On smaller streams with steeper slopes, closer spacing should be the rule. For urban situations, a section every few hundred feet (100 m) or less is often needed. (Dyhouse et al., 2003).

Through several years of experience with dynamic routing models in numerous applications and by using numerical convergence testing for a wide spectrum of unsteady flow applications, Fread (1993) developed an empirical selection criterion between the time step and the hydrograph time of rise:

$$\Delta x \leq \frac{cT_r}{20} \tag{21}$$

where: T_r is the hydrographs time of rise in hours (T).

c is the bulk wave speed (the celerity associated with an essential characteristic of the unsteady flow such as the peak or the center of the hydrograph) in km/hr (L/T).

In most applications the bulk wave speed is approximated as the kinematic wave speed. The kinematic wave celerity is approximated as:

$$c = kv \tag{22}$$

where: k is the kinematic wave ratio having values ranging from $4/3 \leq k \leq 5/3$

$k \approx 1.5$ for most natural channels

v is the flow velocity.

Figures 15 and 16 respectively illustrate the observed peak discharge hydrographs at the three major hydrometric stations (Dissangis, Chablis and Beaumont) for the April 1998 and March 2001 floods. The figures also show the wave time of transfer in hours between the three stations. The peak flow velocity during the 1998 peak is 0.48m/s while the 2001 peak flow velocity is 0.6m/s.

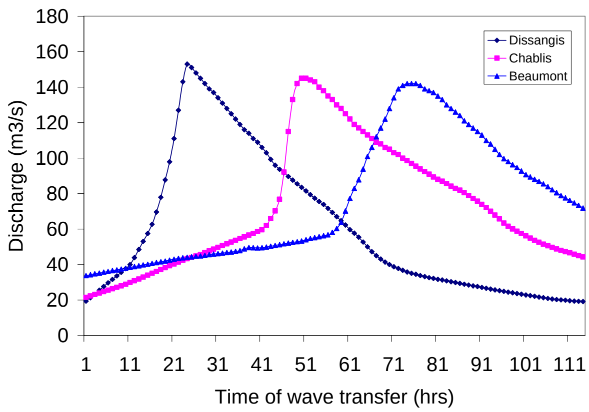

Fig.15 Observed time of wave transfer of the April 1998 flood peak from Dissangis to Beaumont

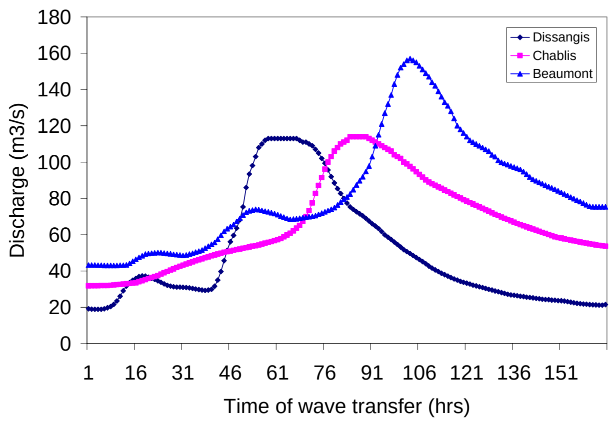

Fig.16 Observed time of wave transfer of the March 2001 flood peak from Dissangis to Beaumont

Because the period of simulation (8years) is too long when compared to classic hydraulic simulations and due to the fact that the input hydrograph contains several peaks with wave transfer time differing in accordance to the intensity and hydrological properties of the flood, it was difficult to obtain numerical convergence depending on the above Δx selection criteria. A wide spectrum of convergence tests was conducted to select the most appropriate Δx. Large distance steps ($\geq 1000m$) created numerical oscillations and failure in matrix solution in periods of high flow. The Δx of 250m found to be stable in both high and low flow simulations, however numerical oscillations occurred when conducting sensitivity analysis on Manning's roughness coefficient. The Δx of 100m was the most stable distance increment and therefore adopted in all model simulations and sensitivity analysis.

5.2 Manning’s roughness coefficient (*n*) calibration

Manning's *n* normally carries the most uncertainty in a hydraulic model. In this study a wide range of possible Manning’s roughness coefficients values for both the main channel and floodplain are investigated to calibrate the model.

The calibration of *n* was investigated at Chablis Station where observed water level and discharge hydrographs are available. The *n* of main channel was varied from 0.01 to 0.05 at $\Delta n = 0.002$, and from 0.05 to 0.1 at $\Delta n = 0.01$. The Increase in Manning’s roughness coefficients in the main channel had the following impacts on the simulation: a) Local increase in stage in the area where the Manning’s n values were increased b) Decrease (attenuation) in Peak discharge has happened as the flood wave moves downstream, c) Increase of travel time d) The loop effect is wider (i.e. the difference in stage for the same flow on the rising side of the flood wave as the falling side will be greater).

The *n* of floodplain was varied from 0.02 to 0.2 at $\Delta n = 0.01$. The variation of *n* in the floodplain did not influence the results at Chablis; this is due to the fact that no overtopping has occurred in Chablis section during the period of simulation. The slight overtopping upstream of Chablis seemed to have no influence on the simulated stage and discharge hydrographs at Chablis when using higher values of *n* in the floodplain. For this reason the floodplain plain was given the same values of the main channel.

The value of $n = 0.028$ is found to be the optimal value of the Serein River model because it gave the best results when comparing the simulations to observations at Chablis. The performance of the model at Chablis was statistically evaluated at table 4, while the comparison between observed and simulated discharge and water level hydrographs is illustrated respectively in figure 17 and figure 18.

Table 4. Model performance at Chablis

	Avarege observed	Average Simulated	Determination Coef. (Nash)	Bias %	RMSE	Correlation coefficient
Q (m3/s)	8.6 m3/s	8.37 m3/s	0.904	-2.67 %	3.72 m3/s	0.954
WL (m)	131.49 m	131.57 m	0.896	0.011%	0.15 m	0.955

The accuracy of calibration at Chablis is considered good, considering the range of flows included and the uncertainties of simulated lateral inflows. Using different friction coefficients for different river segments between Chablis and Beaumont may improve the calibration, but as there are no reference points for this reach, no justification for the use of different individual friction values can be given.

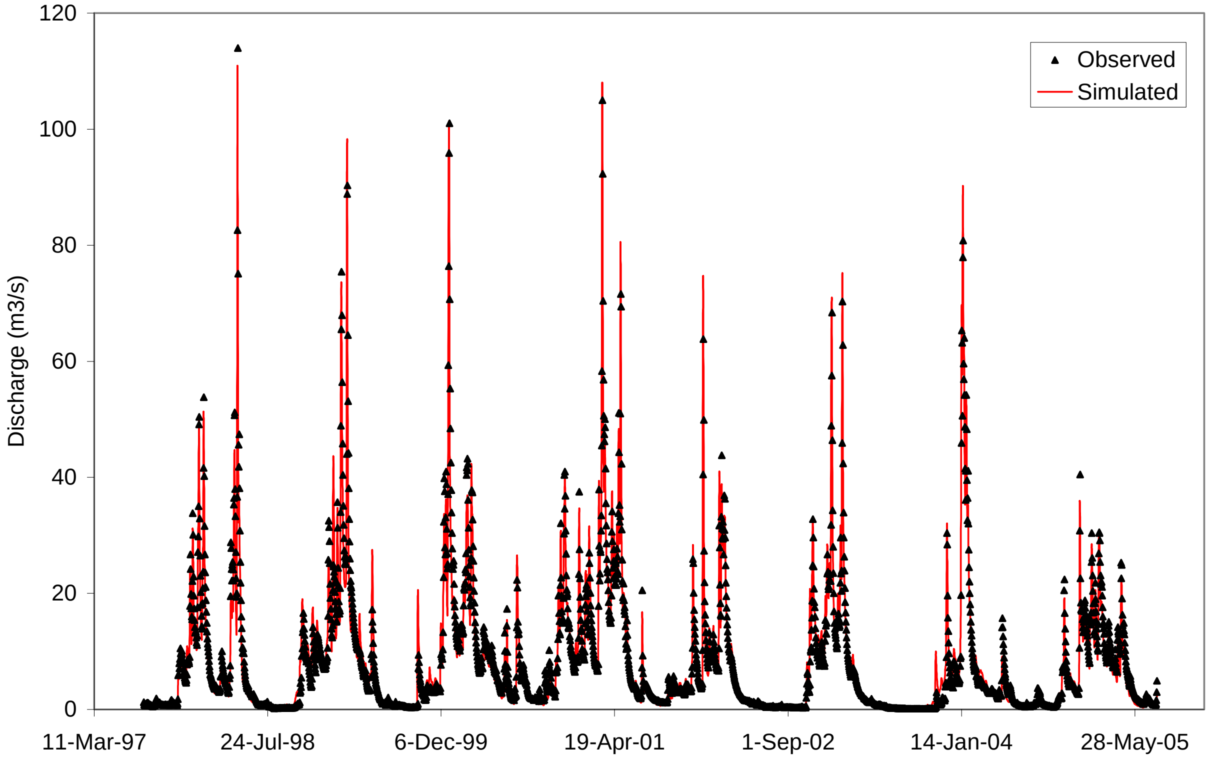

Fig.17 Model discharge calibration at Chablis

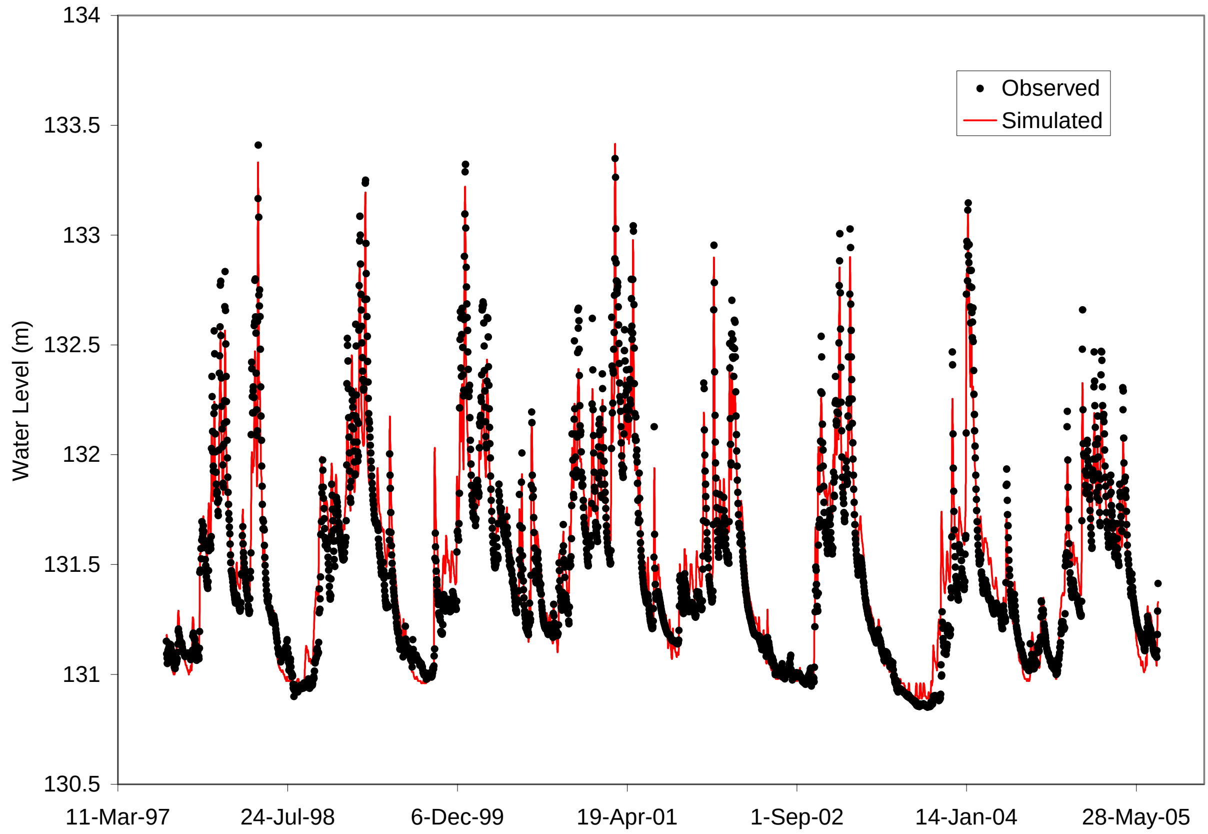

Fig.18 Model water levels calibration at Chablis

6 Geometry Sensitivity

The morphology of alluvial channels has attracted the attention of researchers since early this century (e.g., Lindley, 1919).

Hydraulic geometry has a controlling influence on the shape of flood waves and velocity (Western et al., 1997) and sediment transport capacity (Richards, 1982; Chang, 1988) which is strongly linked to the transport of nutrients and other pollutants. Hydraulic geometry also influences the movement of water, sediments and nutrients between the channel and floodplain through overbank and subsurface pathways.

Regional variation in the size and shape of river channels has been the core concern of fluvial geomorphologists for decades. Such variation is also of interest for hydrologists for flood routing (e.g. Snell and Sivapalan., 1995) and stream ecologist looking at the longitudinal distributions of habitats along a river (Gordon et al., 2004).

Effective catchment-scale management of flooding, floodplains, sediment and nutrient transport, and river habitats requires the evaluation of variations in hydraulic geometry throughout river networks (Stewardson, 2004).

Variability in river hydraulic geometry throughout stream networks is central to the problems of catchment management because of its influence on flow and sediment routing, physical habitats and channel-floodplain interactions (Stewardson, 2005). Variability or irregularity in stream channel cross-sections and channel slope can also be important in other types of stream. For example, in pool-riffle streams, the hydraulic behavior at low flow is dominated by backwater effects resulting from features such as bars (Miller and Wenzel. 1985; Hey, 1988). In effect, the variability in the channel increases the range of flow velocities and water depths which occur in a stream reach (Western, 1994), thereby increasing the diversity of the physical habitats in the stream (Rabeni and Jacobsen, 1993; Gubala et al., 1996).

Natural streams are characterized by variations in cross section and bed slope along their channels. These changes occur over a range of different spatial scales and have both systematic and stochastic components. These variations result from several interacting features of the river system including the discharge characteristics, the quantity and characteristics of sediment load, and the perimeter (bed and bank) sediments that form the channel boundaries (Leopold et al., 1964).

From a hydraulic perspective, channel variability is significant because it causes changes in the hydraulic conditions (width, depth and velocity), especially during periods of low flow, and because it influences flow resistance. The irregular bed slopes and cross-sectional shapes found in natural channels give rise to irregular pressure and gravity forces in the flow direction. Thus, channel irregularities can be thought of as producing an irregular driving force (Chiu and Lee, 1971). Li et al. (1992) considered these irregular inputs from a stochastic perspective and, using a stochastic version of the steady state momentum equation, have shown that flow resistance in open channels is always increased by large-scale irregularity. This effect is most significant for low Froude numbers (which usually occur during low flows) and is small for high Froude numbers (Li et al., 1992).

At the catchment scale there is a tendency for width, depth, and therefore cross sectional area, to increase downstream, and for the width to increase more quickly than the depth. These trends are associated with a downstream increase in discharge (Leopold et al., 1964, P. 202). Since the width increases more quickly than the depth there is a scale dependence in the cross sectional shape (Richards, 1982). There is also a tendency for the channel slope to decrease downstream which leads to a concave longitudinal profile (Leopold et al., 1964; Richards, 1982).

Based on these characteristic, simple cross-sectional hydraulic geometry relations were introduced by Leopold and Maddock (1953) to describe the hydraulics of river cross-sections and variation in channel dimensions throughout river networks. Leopold and Maddock (1953) introduced the term **'at-a-station hydraulic geometry'** to describe empirical relations between width (W), mean depth (D) and mean velocity (U) at a cross-section of a stream channel and discharge (Q). These relations commonly take the form:

$$W = aQ^{b} \tag{23}$$

$$D = cQ^{f} \tag{24}$$

$$U = kQ^{m} \tag{25}$$

The six parameters (a, b, c, f, k and m) are normally estimated by regression using surveys of hydraulic conditions at a cross-section at two or more discharges. To maintain dimension the sum of the exponents (b+f+m) and the product of the constants (a,c,k) must equal one.

Yet, there is no theoretical argument for the use of power functions (Rhoads, 1992), rather this selection is based on empirical analysis (Leopold and Maddock, 1953). Leopold and Maddock (1953) also introduced downstream hydraulic geometry relations taking the same functional form as Eqs. (1)-(3) but relating channel width, depth and velocity at bankfull to mean discharge along a river channel. Others have since used the bankfull discharge, instead of the mean discharge, as the independent variable in these downstream hydraulic geometry relations (Harman et al., 2008)

Recently, there have been efforts to develop hydraulic geometry relations for the distribution of cross-sectional hydraulic parameters within a reach based on surveys of multiple cross-sections. Some studies have examined the variability of channel geometry for studies of fluvial processes (Western et al., 1997; Buhman et al., 2002), others have developed hydraulic geometry relations for reach-averaged hydraulic parameters to assist stream habitat assessment (Singh and McConkey, 1989; Jowett, 1998; Lamouroux and Suchon, 2002; Lamouroux and Capra, 2002).

This determination of hydraulic geometry relationships through river networks provides important inputs to regional scale hydrological models for predicting flood frequency and extent, pollutant transportation, sediment and nutrient throughput and ecosystem conditions, e.g., (Prosser et al., 2001a), (Lu et al., 2004), (McKergow et al., 2004) and (DeRose et al., 2005).

An important geomorphological factor to achieve successful inundation simulations is the correct identification of the bankfull stage and discharge. Bankfull stage corresponds with the discharge that fills a channel to the elevation of the active floodplain. The correct identification of the bankfull stage in the field can be difficult and subjective (Williams, 1978; Knighton, 1984; and Johnson and Heil, 1996).

Numerous methods exist for bankfull stage identification in the field (Wolman and Leopold, 1957; Nixon, 1959; Schumm, 1960; Kilpatrick and Barnes, 1964; and Williams 1978). Field indicators of bankfull stage include significant breaks in slope, changes in vegetation, the highest scour line, or the top of the bank (Leopold, 1994).

In hydraulic models based on the Saint Venant equations it is well-known that river flow is influenced by several cross sectional morphological factors, among which the channel slope and the cross sectional representation of the geometry. However the literature does not show to what extent these morphological factors influence the quality of the hydraulic model in predicting water levels and discharge hydrographs.

Over the last two decades the linking between hydraulic models and Geographic Information Systems (GIS) has been a major development in flood modeling. In 1988 Jenson and Dominique have suggested an approach to delineate watershed boundaries and stream networks using geographic information extracted from Digital Elevation Models (DEM). Later studies (e.g. Andrysiak et al., 2000) combined the Hydrologic Engineering Center's Hydrologic Modeling System (HEC-HMS) and Hydrologic Engineering Center's River Analysis System (HEC-RAS) with GIS to develop a model that accurately represents floodplains.

Although DEMs provide sufficient data for watershed delineation purposes and floodplain representation, they usually lack the accuracy required to represent stream channel details. An example that illustrates this problem is shown in figure 19, where we compare a cross section of the Serein River that is obtained from two different methods. The first cross section is obtained by geological surveys (source: DIREN) while the other is obtained from a DEM (75m resolution) .The floodplain is rather well presented in the section obtained from the DEM with a correct minimum altitude even if the width is underestimated, but the digital terrain data does not contain information about the main channel.

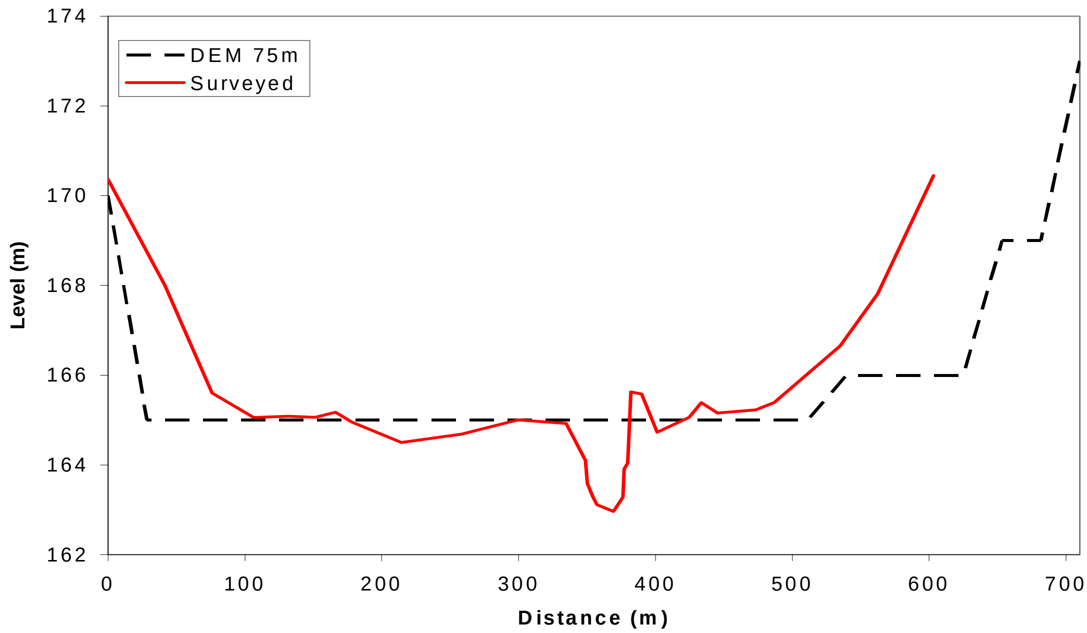

Fig. 19 Comparison between a DEM and surveyed cross section along the Serein River

To investigate the influence of minimum field data available on the hydraulic model, the objective of this part of study is to examine the sensitivity of the hydraulic model to the river geometry. Also attempt to explore the validity of using simplified geometry in areas where surveyed cross sections are not available, since the principal objective of this thesis is to simulate water level and discharge hydrographs on a regional scale where surveyed cross sections are not always available.

To achieve this objective, several "what if" geometry scenarios are tested. Table 5 describes briefly the scenarios considered for this sensitivity analysis and their main objectives.

Table. 5 Scenarios of river geometry

Scenario	Description	Objective
I	Replacing each irregular surveyed section by a regular trapezoidal section that has equivalent area, depth and width of the surveyed section.	Test the sensitivity of simulated water level and discharge hydrographs to the irregularity of cross sections representing the main channel.
II	Removing cross sections that contain two conveying arms (islands)	Evaluate the importance of detailed river geometry and its influence on the quality and numerical convergence of the model.
III	Only three surveyed cross sections (located at major hydrometric stations) are used to represent the geometry of the river.	Importance of spatial distribution of cross sections if discharge and water levels hydrographs are required in several locations along the river reach.
IV	Generalizing only one surveyed cross section along the river reach. Three different tests were conducted by using the Sections at Dissangis, Chablis and Beaumont.	Test the quality of simulated water level and discharge hydrographs to the representation of geometry using a single uniform surveyed cross section.
V	Representing the river geometry by a trapezoidal section obtained from average surveyed information.	Test the sensitivity of simulated water level and discharge hydrographs to the cross sectional shape representation of geometry and interpolated bed level slopes.
VI	Representing the river geometry by a triangular section obtained from average surveyed information.	
VII	Representing the river geometry by a rectangular section obtained from average surveyed information. Followed by the recalibration of Manning's n to improve results	
VIII	Excluding the floodplains from the model and using only surveyed main channels to represent the river geometry. In case of overtopping, bank walls will be extrapolated vertically.	Examine the sensitivity of simulated water level peaks to the presence of floodplain. The test also aims at identifying the attenuation in water levels of a composed channel (main channel + floodplain) compared to that obtained by only using the main channel geometry.

All geometry scenarios use the hydraulic computational parameters illustrated in table 6. These hydraulic computational factors were obtained through calibrating the Serein River model (section 5).

Table. 6 Hydraulic computational parameters used in river geometry scenarios

Upstream Boundary Condition	Lateral inflows	Downstream Boundary Condition	Δt (computational time step)	Δx (computational distance step)	θ (Implicit weighting factor)	n_c (Channel roughness coefficient)	n_f (floodplain roughness)
Observed Discharge Hydrograph	Simulated by MODCOU	Rating Curve at Beaumont	1 hr	100 m	1	0.028	0.028

The results obtained from different "what if" scenarios are compared with observed water level and discharge hydrographs at Chablis. Results are also compared longitudinally with the discharge, water levels and maximum water depth obtained by the reference simulation. The reference simulation in this report refers to results obtained using the most documented river geomorphological data.

6.1 Scenario I : Replacing each irregular surveyed section by an equivalent regular trapezoidal section

This scenario aims at testing the sensitivity of simulated water level and discharge hydrographs to the simplification of the cross section geometry of the main channel.

The surveyed main channels (irregular sections) were replaced by trapezoidal sections (regular sections). The wetted area, depth and bankfull width properties of each irregular section were used to construct the uniform trapezoidal section, additionally the irregular channel properties were used to identify the bottom width and side slope of the trapezoidal section. The geometry of the floodplain is kept unchanged. An example of this main channel modification is illustrated in figure 20.

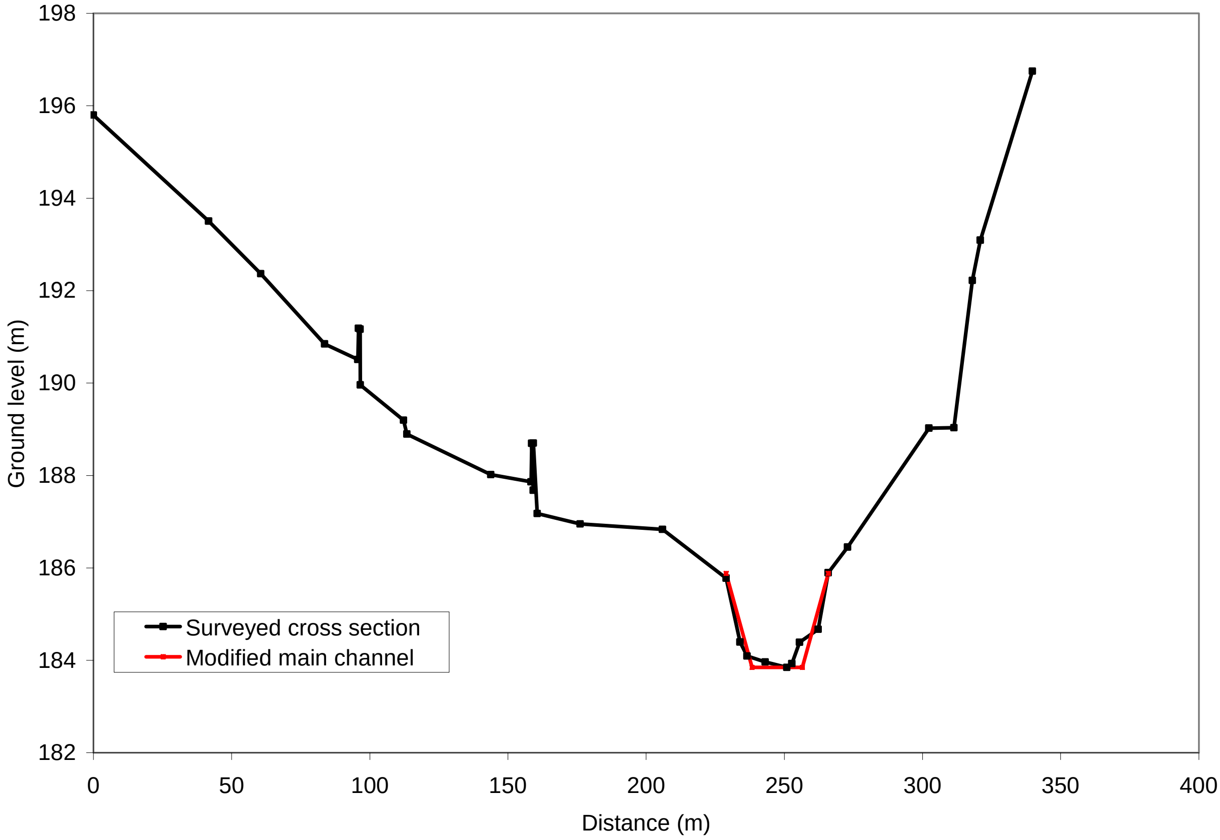

Fig. 20 Example of main channel modification from irregular to regular shape

Comparison of Nash with the reference simulation is illustrated in figure 21. The Comparison illustrates that simulated discharge hydrographs are not influenced by this geometry scenario. A sharp influence was remarked in simulated water levels of certain cross sections, it was also noticed that low flow periods are more sensitive than high flow periods to this geometry scenario. This is due the fact that as the water level of the regular section approaches the bankfull level, the hydraulic characteristics of the regular section becomes equal to the hydraulic characteristics of the irregular sections:

If $Y_r = Y_{bf}$, then $A_r = A_{ir}$, $T_r = T_{ir}$

where: *Yr* is the water level in the regular channel

Ybf is the bankfull water level

A is the wetted cross sectional area

T is the top width

Subscripts *r* and *ir* stand for regular and irregular sections

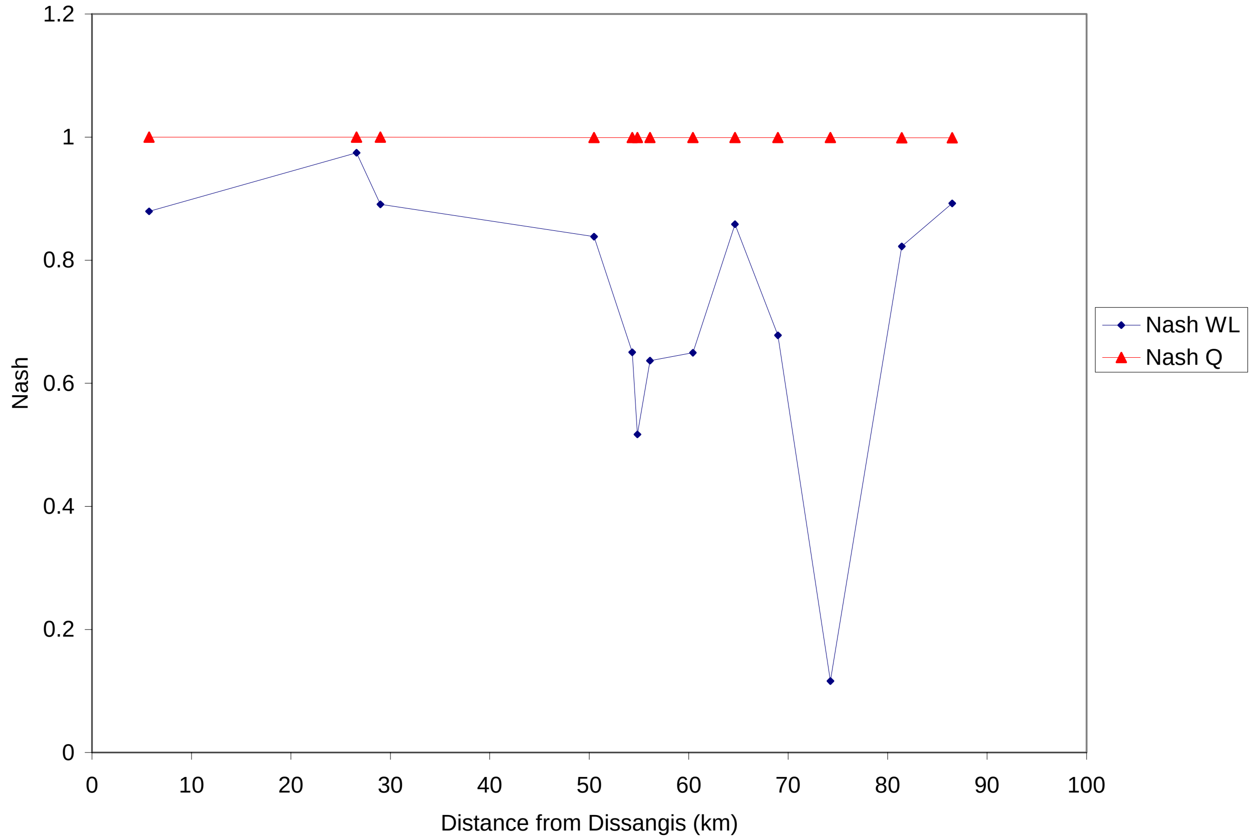

Fig. 21 ***Nash statistical index between the simulation of reference and simulations obtained from the trapezoidal section***

Through the Nash comparison, the less accurate results were found at section 3, located at 74 km from Dissangis (figure 22). The comparison of the water level hydrograph with the reference simulation in section 3 (figure 24) shows the influence of this modification on water depths specially at low flow periods where high irregularities exist in this particular section. These irregularities were neglected by the trapezoidal section, as it considers a plain bottom width. The wetted area as function of water level is compared in figure 23, the comparison exhibits the large difference during low flow periods, the difference between the two wetted areas decrease as the water level rises towards the bank level. An improvement in results might be obtained by varying the manning's roughness coefficient vertically.

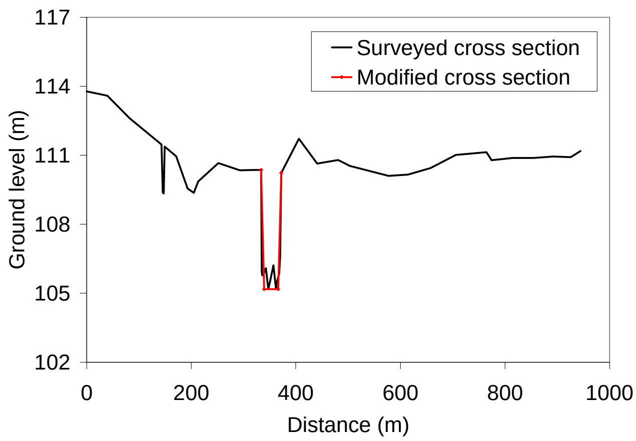

***Fig.22 Surveyed* irregular vs. modified regular shape of section 3**

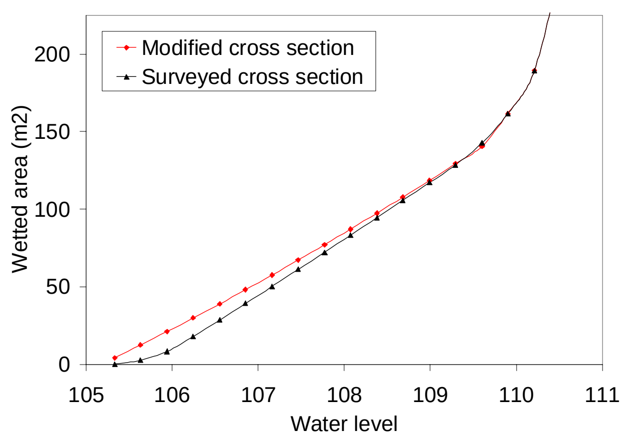

***Fig.23 Surveyed* irregular vs. modified regular wetted area of section 3**

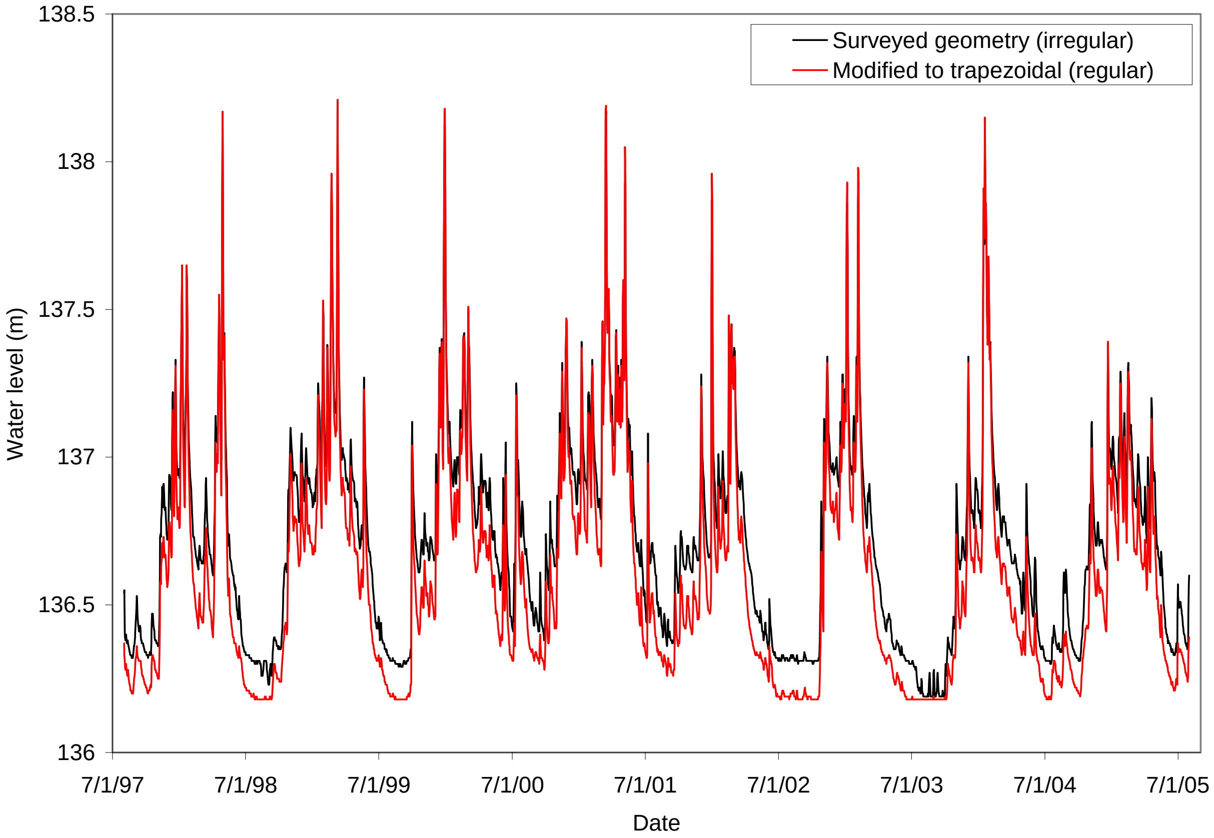

Fig. 24 Comparison of water levels obtained from regular and irregular geometrical shape of section 3

6.2 Scenario II: Removing cross sections that contain two conveying arms (islands)

In this particular scenario, the cross sections containing two conveying channels were removed from the geometry representation of the Serein River. The four cross sections removed from the model (figures 25a and 25b) are as follows:

CS-16 located at 21.89 km from Dissangis
CS-15, located at 26.58 km from Dissangis
CS-12, located at 35.5 km from Dissangis
CS-11, located at 41.57 km from Dissangis
The sections removed were replaced by interpolated sections obtained from adjacent sections.

The main objective of this test is to evaluate the influence of removed sections on the prediction quality and numerical convergence of the model. This test also aims at evaluating the importance of detailed river geometry in the hydraulic model

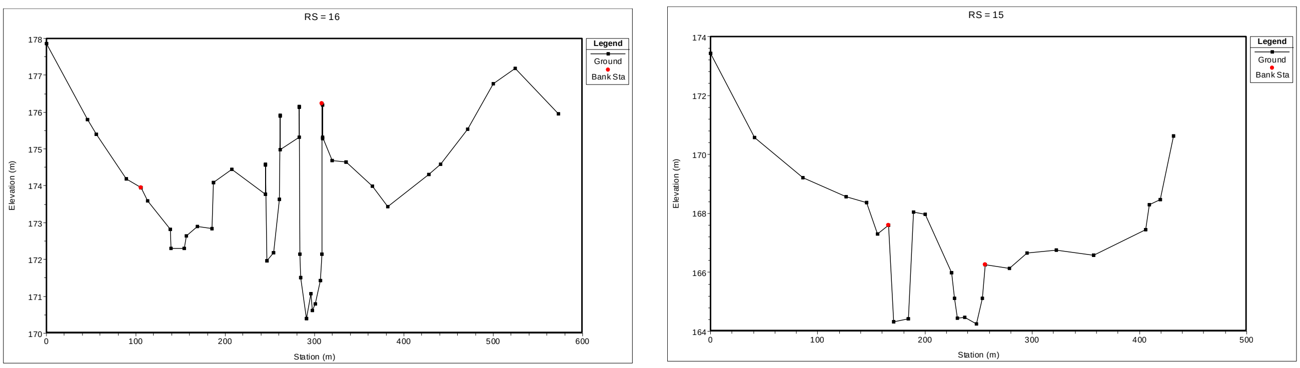

Fig. 25a Removed cross sections 16 & 15 from the geometry representation of the Serein River

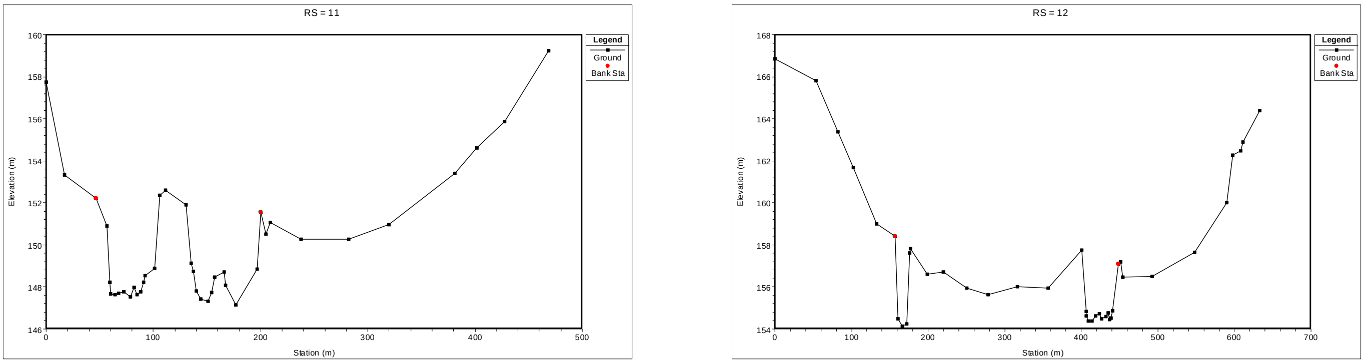

Fig. 25b Removed cross sections 12 & 11 from the geometry representation of the Serein River

The results obtained from this scenario demonstrate that maximum water depths were influenced in locations where cross sections were removed (figure 26). The removal of the sections had no influence on the wave time of transfer and produced discharge hydrographs, it should also be mentioned that simulated water levels and discharge hydrographs at Chablis were not influenced by the removal of these sections. In terms of numerical convergence, the model with no islands was more stable than the original model and allowed us to use spatial computational steps that are equal or larger than 2 km. The test exhibits the importance of using accurate cross sections where water levels are required.

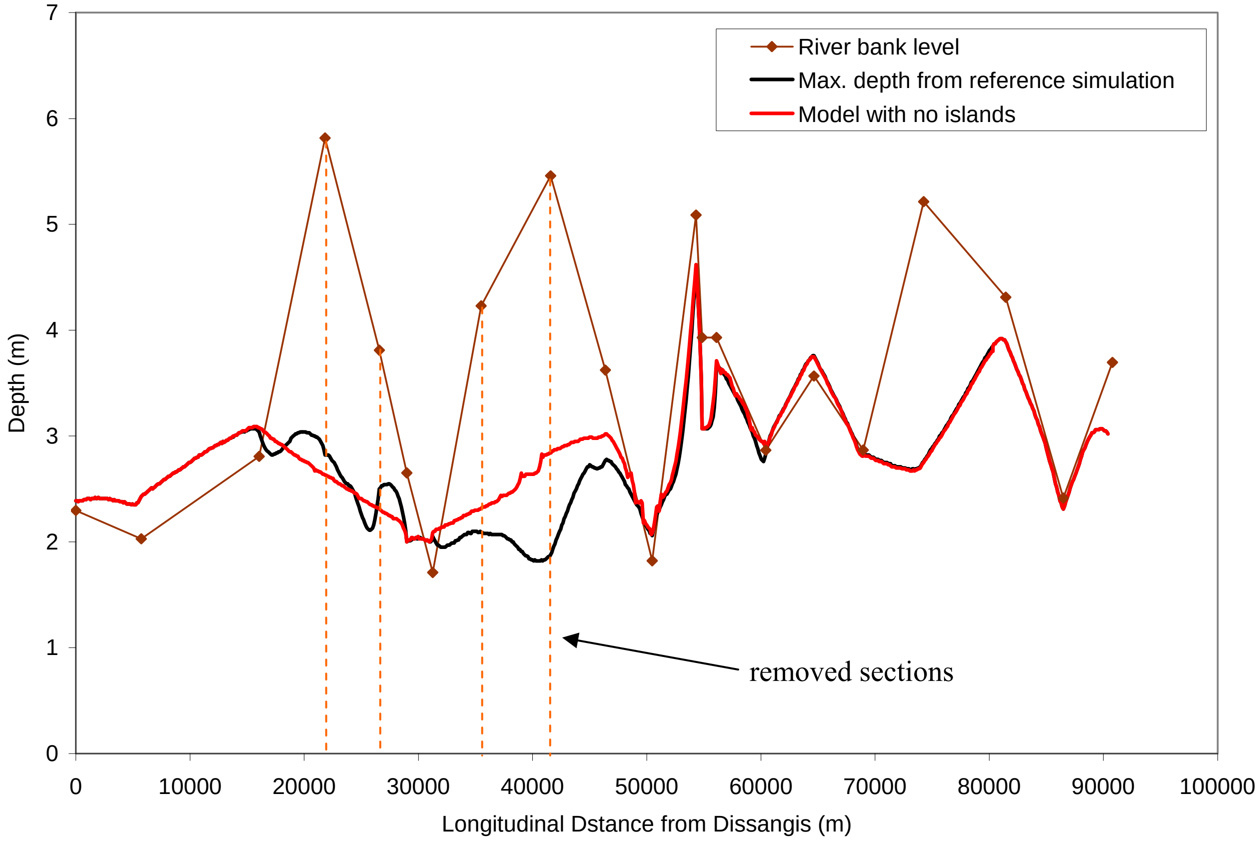

Fig. 26 Longitudinal comparison of maximum water depths between the simulation of reference and scenario II

6.3 Scenario III: Only three surveyed cross sections used to represent the geometry of the Serein River

This scenario evaluates the prediction of the model when representing the river geometry with only three surveyed cross sections. These surveyed sections are located at major hydrometric stations (Dissangis, Chablis, and Beaumont) where geometry is routinely checked. Linear interpolation proposed by preprocess of HEC-RAS was used to generate additional sections at a distance step of 100m along the Serein River. Cross sections bed levels were linearly interpolated between the three known bed levels of surveyed sections.

The performance of the model is illustrated in table 7. The statistical criterions (Nash and root mean square error) exhibited acceptable results when compared at Chablis station. The model did not accurately represent the maximum water depths when compared longitudinally to the maximum water levels obtained from the reference simulation (figure 27). Results of this scenario illustrates the importance of using several surveyed cross sections for a given river reach, especially whereas sudden change in the cross section shape and bed level slope occur. It also illustrates that comparing the prediction of the model with observations at one single point is not enough to evaluate the accuracy of the model.

Table.7 Model performance at Chablis

Nash WL	Nash Q	RMSE WL (m)	RMSE Q (m^3/s)
0.86	0.89	0.18	3.98

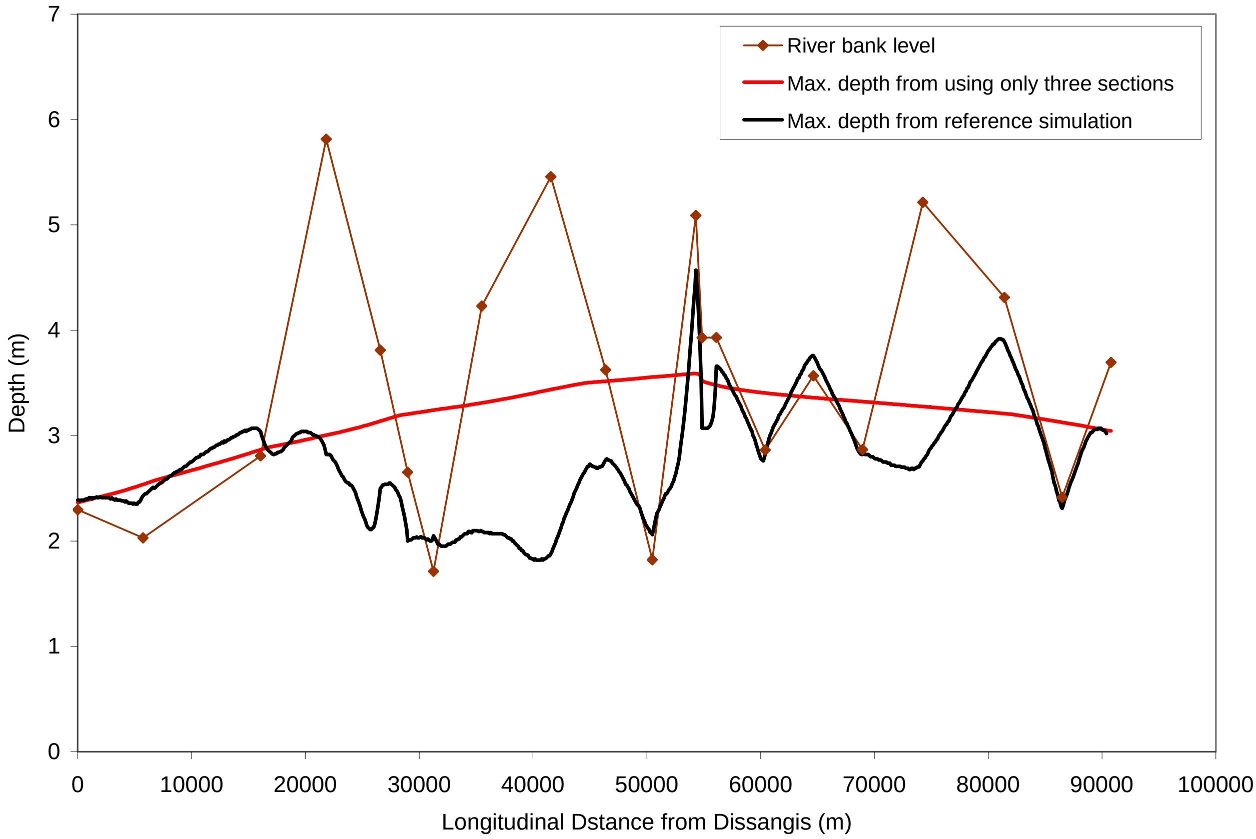

Fig. 27 Longitudinal comparison of maximum water depths along the Serein River

6.4 Scenario IV: Uniformly generalizing one surveyed cross section along the river reach

The scenario tests the sensitivity of simulated water level and discharge hydrographs to the representation of geometry using a single surveyed cross section. The single section is interpolated at constant distance steps (100m) in order to be generalized along the river reach.

Three tests were conducted in this particular scenario, the first test was conducted by generalizing the surveyed cross section at Dissangis, the second test uses the surveyed cross section at Chablis, while the third test uses the surveyed section at Beaumont. The comparison of the three cross sections shapes is illustrated in figure 28.

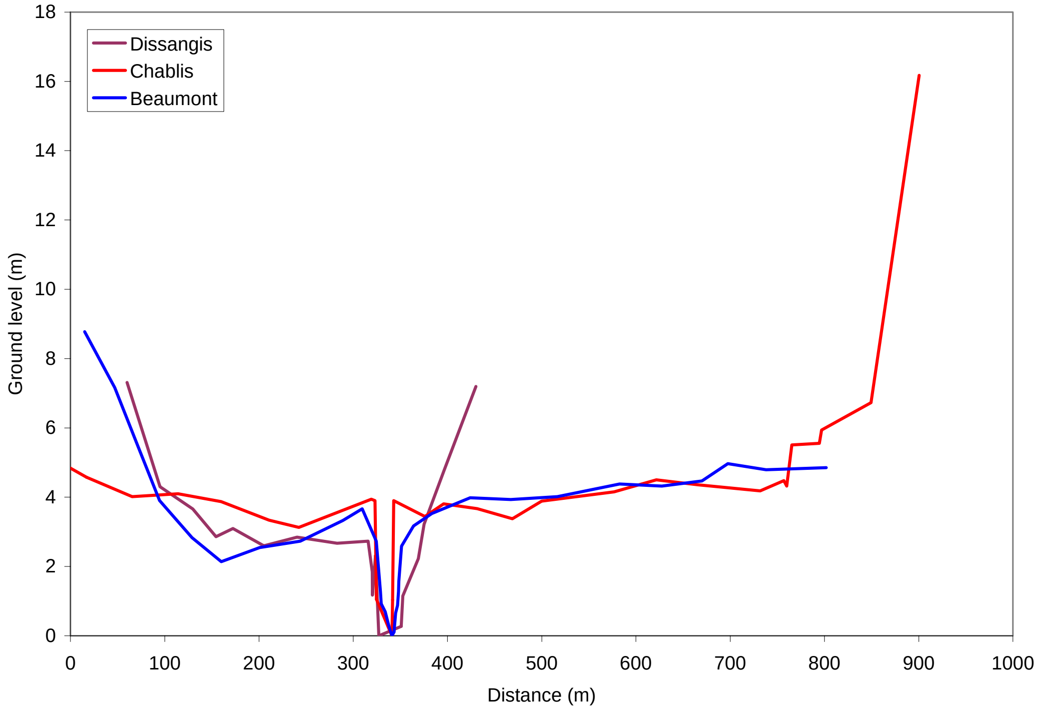

Fig. 28 Comparison between the Dissangis, Chablis and Beaumont cross sections

In all three tests bed levels were interpolated linearly between the three major hydrometric stations using available information on bed levels. The area and wetted parameter hydraulic characteristics of three cross sections are compared at figure 29 and 30. The comparisons of hydraulic properties demonstrate that the area and conveyance of the Serein River cross sections do not depend on the catchment area that they represent. The main river section at Dissangis which represents a catchment area of 643 km^2 had larger conveying capacity and width than Chablis (1120 km^2) and Beaumont (1337 km^2). Sections at Chablis and Beaumont had very close hydraulic properties at main channels.

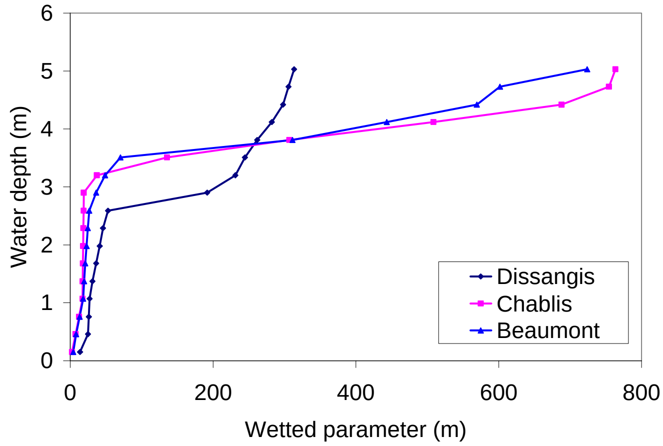

Fig. 29 Comparison between Dissangis, Chablis and Beaumont cross sectional wetted parameter

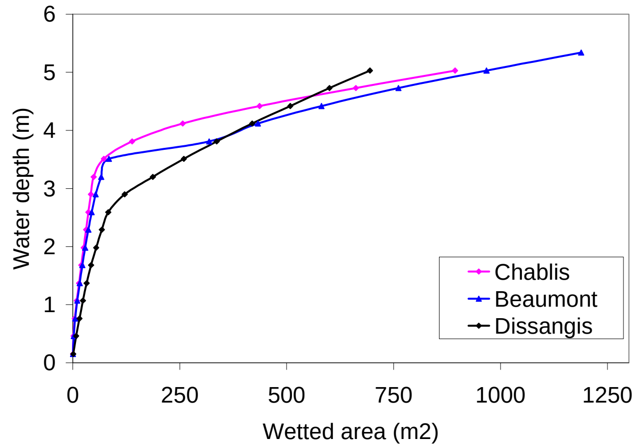

Fig. 30 Comparison between Dissangis, Chablis and Beaumont cross sectional wetted area

The Comparison of simulated water level and discharge hydrographs at Chablis is illustrated in figure 31. The performance of each geometry scenario is illustrated in table 8. The results suggests that simulations obtained using a generalized section surveyed at Beaumont were the most accurate.

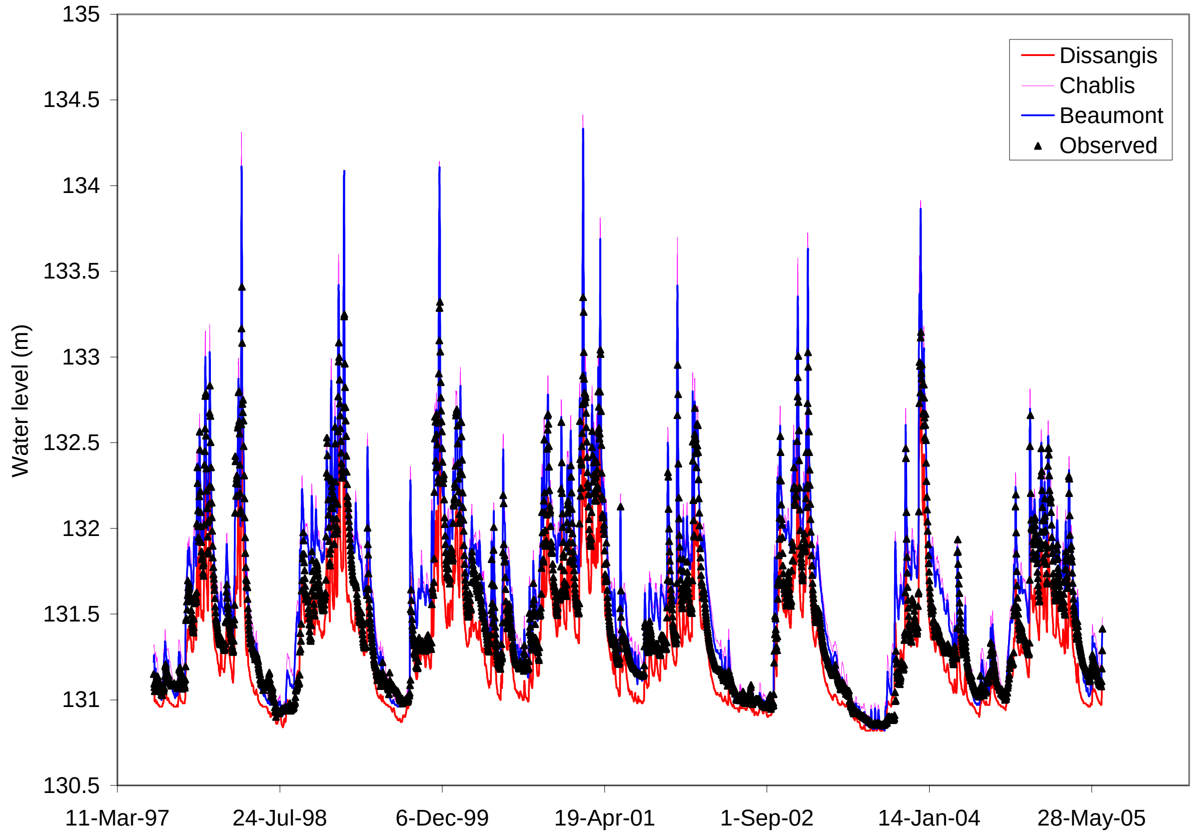

Fig. 31 Comparison of simulated water level hydrographs at Chablis from the three geometry representation scenarios (Dissangis, Chablis and Beaumont)

Table. 8 Statistical comparison of simulated water level hydrographs at Chablis

Section generalized to represent the geometry	Nash WL at Chablis	Nash Q at Chablis	RMSE WL (m) at Chablis	RMSE Q (m^3/s) at Chablis
Dissangis section	0.72	0.89	0.25	3.82
Chablis section	0.69	0.88	0.265	4.12
Beaumont section	0.80	0.90	0.21	3.75

The results suggest that using generalized geometry to represent the river has no influence on simulated discharge hydrographs. The generalized geometry sharply influenced simulated water level hydrographs. The Comparison of maximum water depths are illustrated in figure 32, it shows that generalized geometry influenced the maximum water depths. The longitudinal comparison of maximum water depths shows that both generalized sections of Chablis and Beaumont produced close maximum water depth levels. This is due to the fact that cross sections at Chablis and Beumont have close hydraulic properties as previously shown in figures 29 and 30. The simulations produced using the sections at Dissangis produced lower water depths which is due to the fact the Dissangis cross section has a larger bottom width and different geometric characteristics when compared to Chablis and Beaumont.

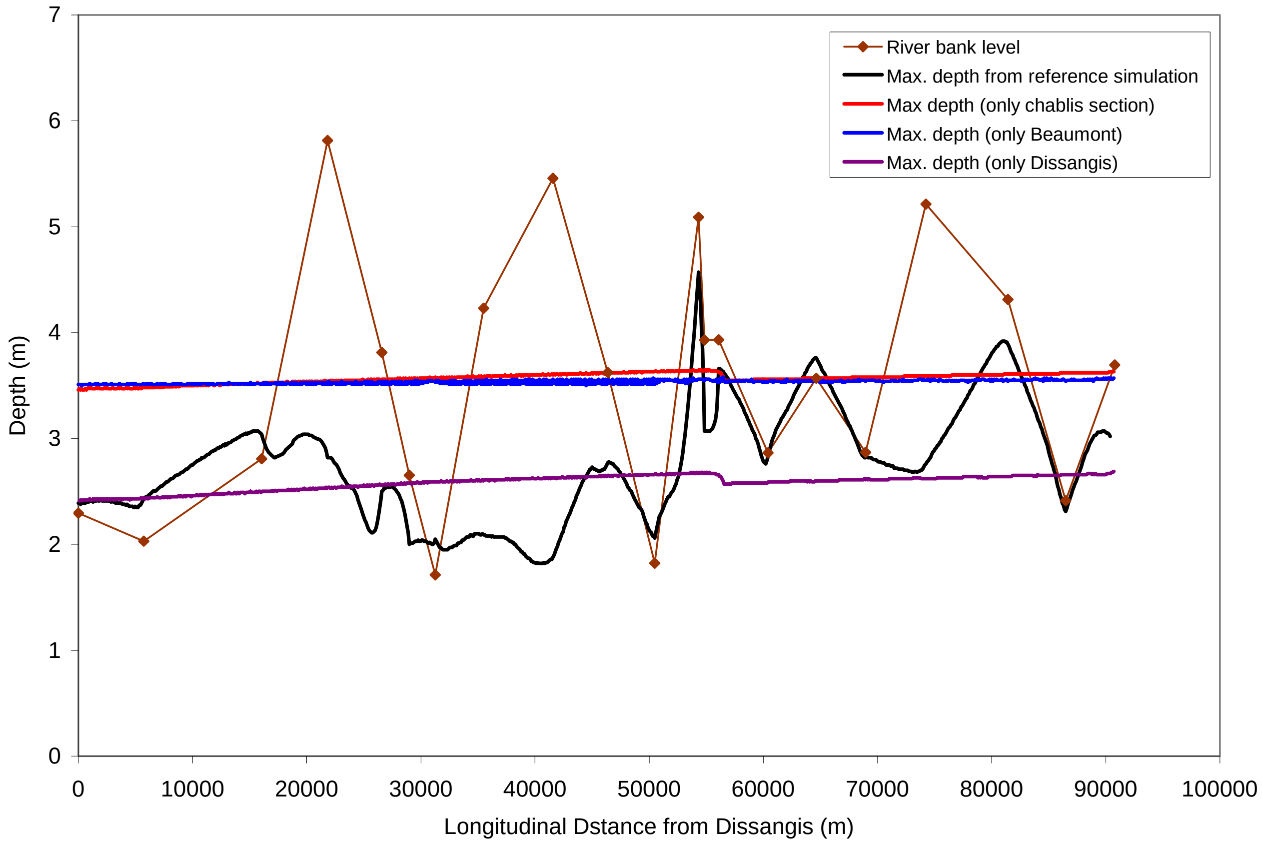

Fig. 32 Longitudinal comparison of maximum water depths along the Serein River

6.5 Scenario V: Representing the river geometry by a trapezoidal section obtained from average surveyed information

This scenario consisted of using the average information obtained from the 20 surveyed cross sections to compose one uniform main channel section. The Average information (depth, width and area) obtained from surveyed main channels was used to assemble a trapezoidal section (figure 33). This trapezoidal section was interpolated at constant distance steps (100m) to represent the geometry of the Serein River.

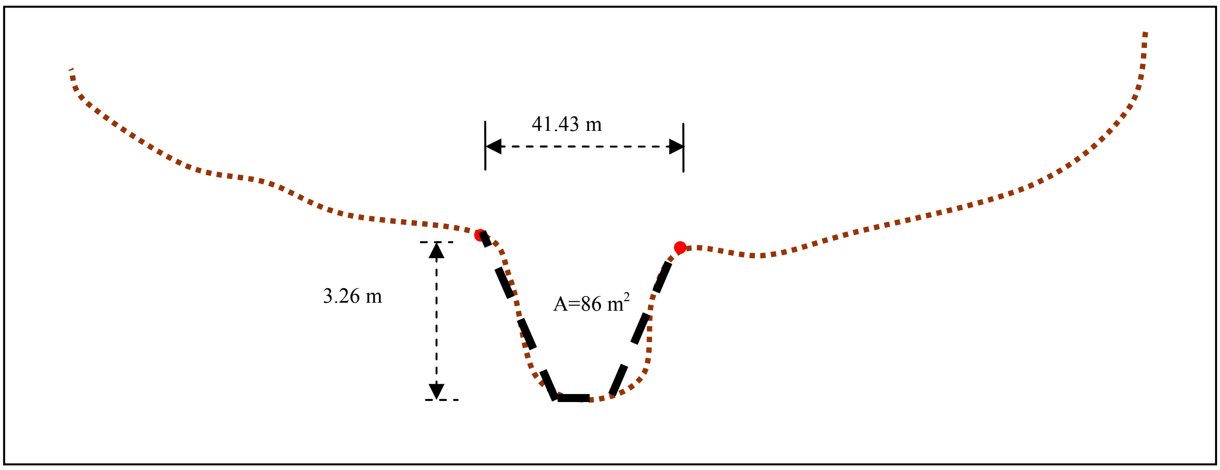

Fig. 33 The trapezoidal cross section obtained from average surveyed information

In this scenario two methods are tested to represent the bed levels of the Serein River. The first method consisted of linearly interpolating the bed levels using only three known bed levels (Dissangis, Chablis and Beaumont), while the second method consisted of using the twenty surveyed bed levels.

The objective from testing these two bed level representation methods is to examine the sensitivity of the model to the bed level slope.

The cut and fill difference in ground levels generated by linear interpolation between the three major hydrometric stations is represented in figure 34. Cut and fill levels varied from + 4 m along the river reach between Dissangis and Chablis, and -2m along the river reach between Chablis and Beumont. The comparison illustrates the non uniformity of bed levels and longitudinal slopes in the Serein River.

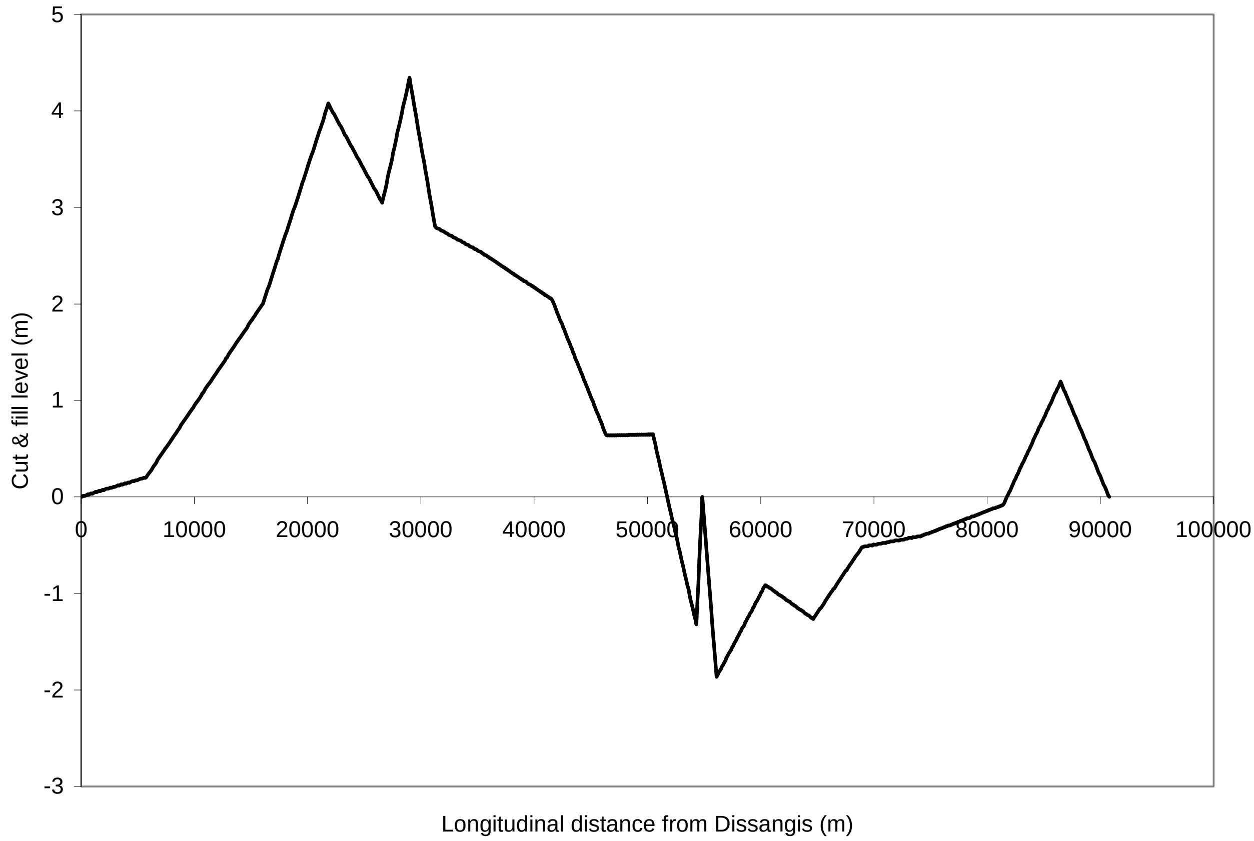

Fig.34 Cut and fill levels generated from the linear interpolation of the bed levels of the three major hydrometric stations

The simulated water levels were first compared with observed values at Chablis station (table 9). The comparison demonstrates the influence of interpolated bed levels on the accuracy of simulated water levels. The discharge hydrographs were not influenced by the bed level slopes.

Table. 9 Statistical comparison of simulated water level hydrographs at Chablis

Bed Level	Nash WL	Nash Q	RMSE WL (m)	RMSE Q m^3/s
20 surveyed bed levels	0.83	0.89	0.19	3.98
3 surveyed bed levels	0.61	0.89	0.30	4

The maximum water depths were longitudinally compared with the reference simulation (figure 35). The comparison exhibits the effect of bed levels on the computed maximum water depths and overtopping frequency, as no overtopping was simulated when using interpolated bed levels.

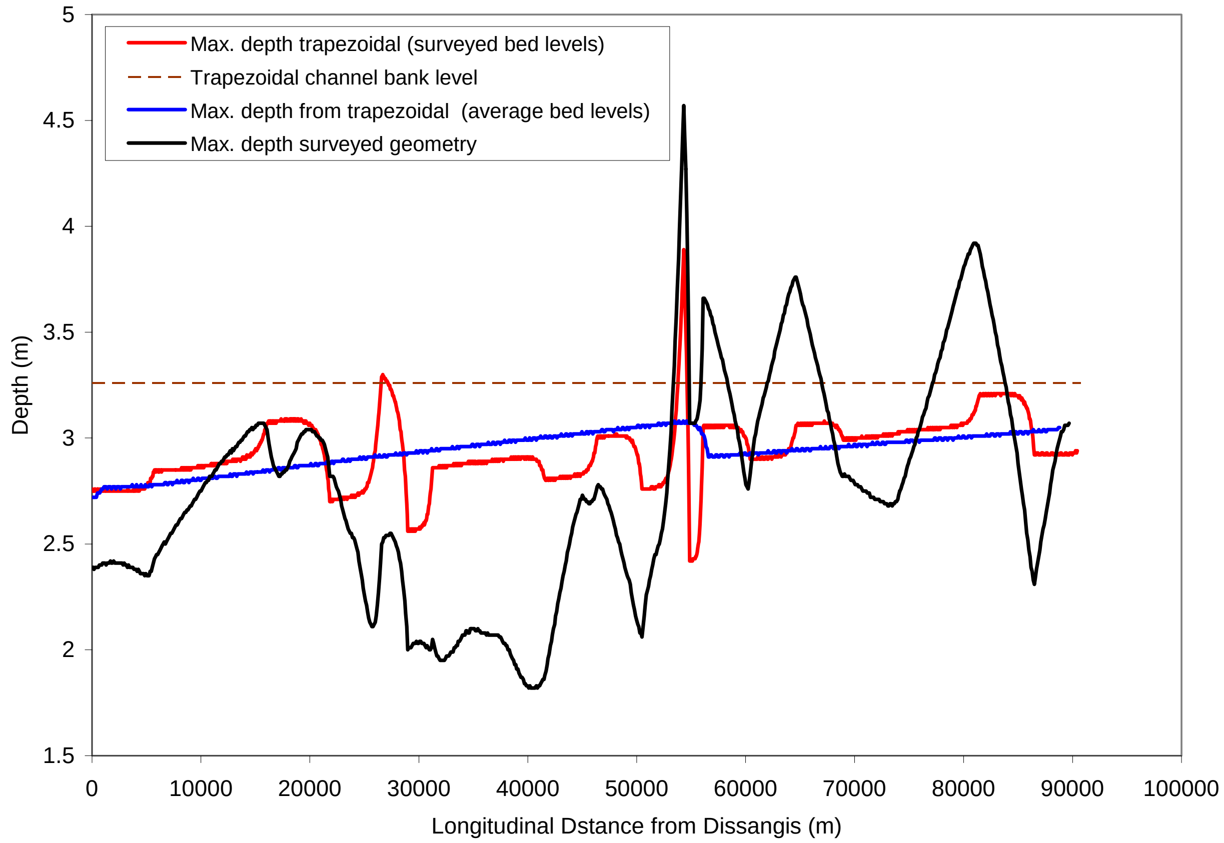

Fig. 35 Longitudinal comparison of maximum water depths along the Serein River

Finally the Nash statistical index was calculated for each cross section by comparing simulations from 20 surveyed bed levels with the reference simulation (figure 36). The comparison demonstrates the influence of cross section characteristics on the simulated water levels in certain sections.

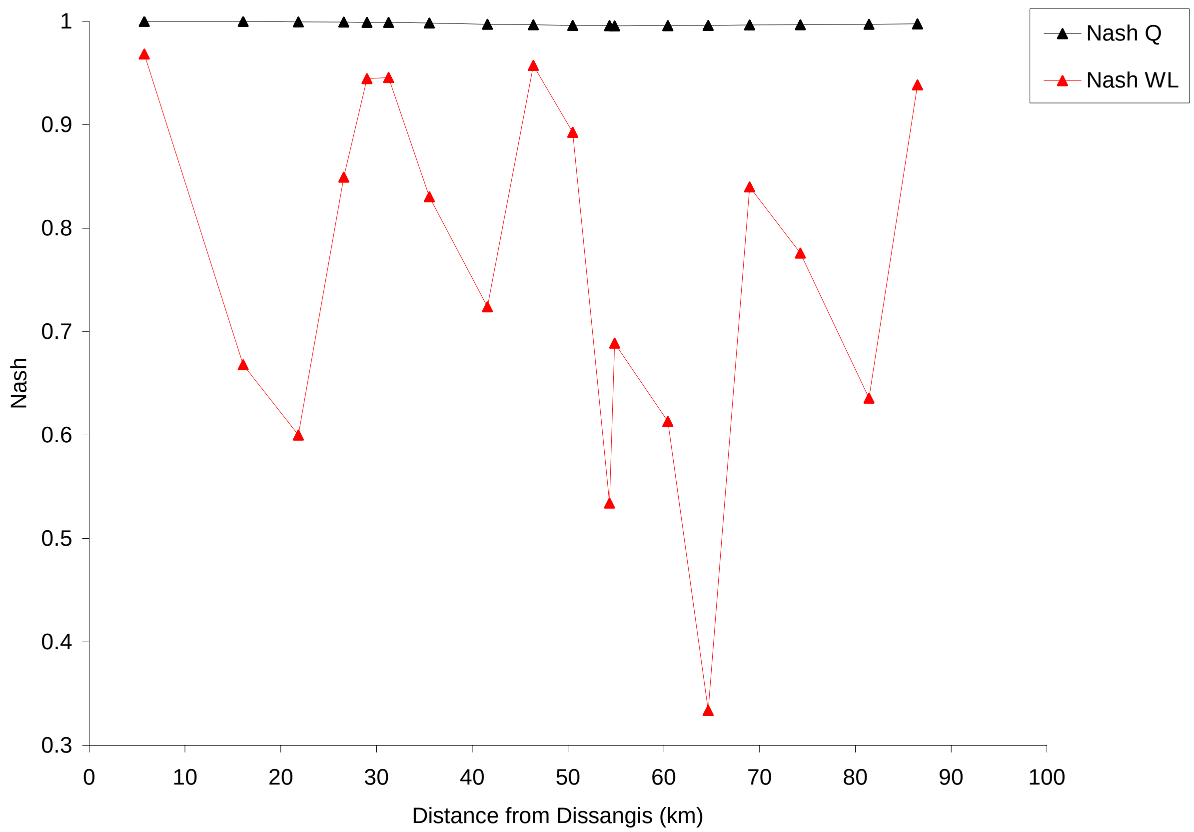

Fig. 36 Nash statistical index between the simulations obtained from the trapezoidal section and the reference simulation

6.6 Scenario VI: Representing the river geometry by a triangular section obtained from average surveyed information.

In this scenario a uniform triangular section is used to represent the river geometry. The dimensions of the triangular section are obtained from the average depth and width of surveyed sections. The bed level slopes are identified by linearly interpolating between the bed levels of the three major hydrometric stations (Dissangis, Chablis and Beaumont).

The simulated water levels are first compared with observed values at Chablis station (table 10). The comparison demonstrates the influence of this geometry scenario on the accuracy of simulated water levels. The discharge hydrographs were not influenced by this scenario.

Table. 10 Statistical comparison of simulated water level hydrographs at Chablis

Nash WL	Nash Q	RMSE WL (m)	RMSE Q m^3/s
0.56	0.89	0.31	3.85

The longitudinal comparison with the reference simulation (figure 37) demonstrates the degradation of simulated water level hydrographs at Chablis and the maximum water depths. Also a back water effect at the downstream end of the reach was remarked. The scenario suggests that it is valid to use simplified geometry for discharge routing and time of wave transfer prediction, but accurate prediction of water levels require accurate river geometry representation.

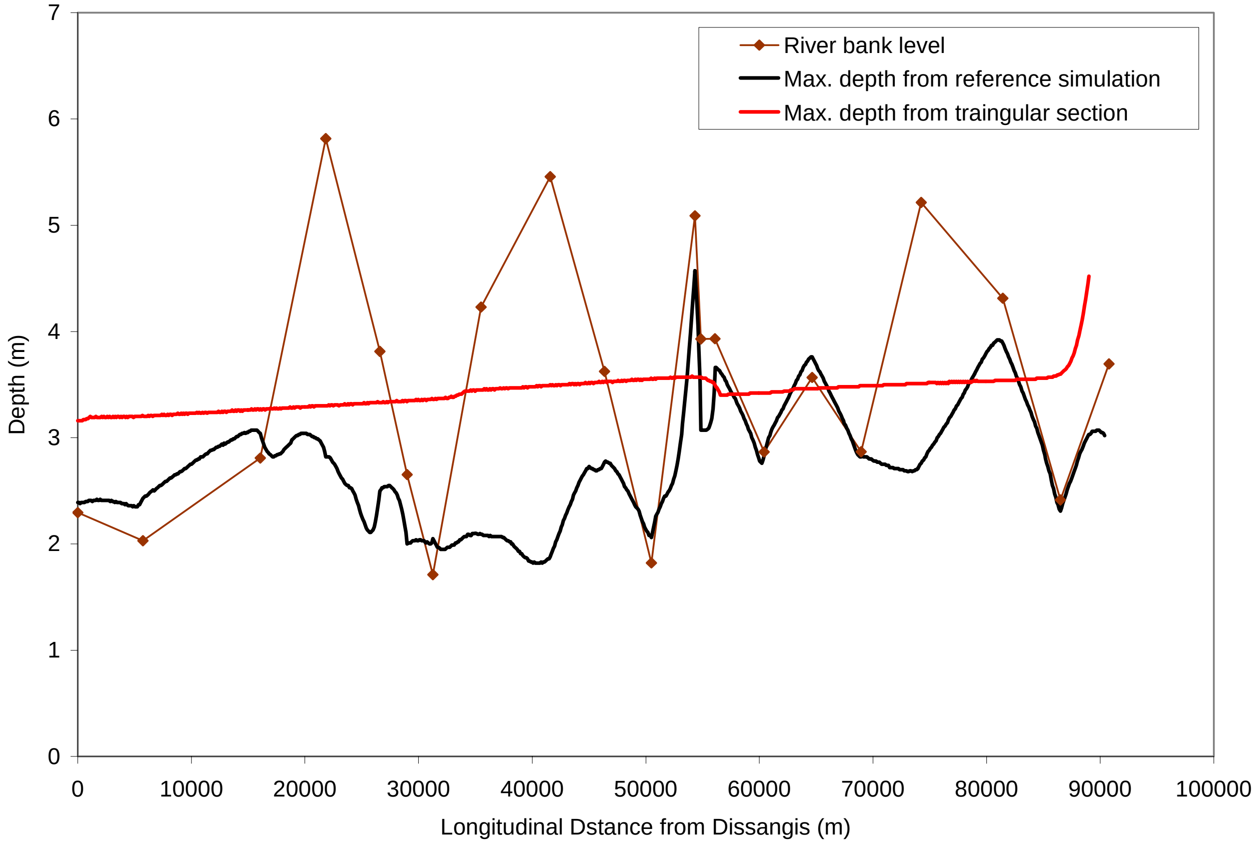

Fig. 37 Longitudinal comparison of maximum water depths along the Serein River

6.7 Scenario VII: Representing the river geometry by a rectangular section obtained from average surveyed information

In this scenario a uniform rectangular channel is used to represent the river geometry. The dimensions of the rectangular section were obtained by using the average depth and area of 20 surveyed cross sections. The bed level slope was identified be linearly interpolating between the bed levels of the three major hydrometric stations (Dissangis, Chablis and Beaumont).

The simulated water levels were first compared with observed values at Chablis station (table 11). The comparison demonstrates the influence of this geometry scenario on the accuracy of simulated water levels. The discharge hydrographs were not influenced by this scenario. For this particular scenario the Manning's roughness coefficient was recalibrated (figure 38). High values of Manning's roughness coefficients were used to improve the prediction of the model at Chablis. According to the Nash statistical index the model prediction improved as Manning's n approaches 0.05.

To validate the approach of recalibrating the manning's roughness coefficient, the recalibrated maximum water profiles were longitudinally compared with the simulation of reference (figure 39).

The comparison showed that the model has been forced to correctly represent the water levels at Chablis and it is not valid for the whole river reach. The recalibrated model also produced errors at the downstream end of the river reach.

Table. 11 Model performance at Chablis

	n=0.03	n=0.04	n=0.05	n=0.06	n=0.07
Nash WL	0.52	0.73	0.837	0.856	0.804
Nash Q	0.88	0.893	0.9	0.916	0.925

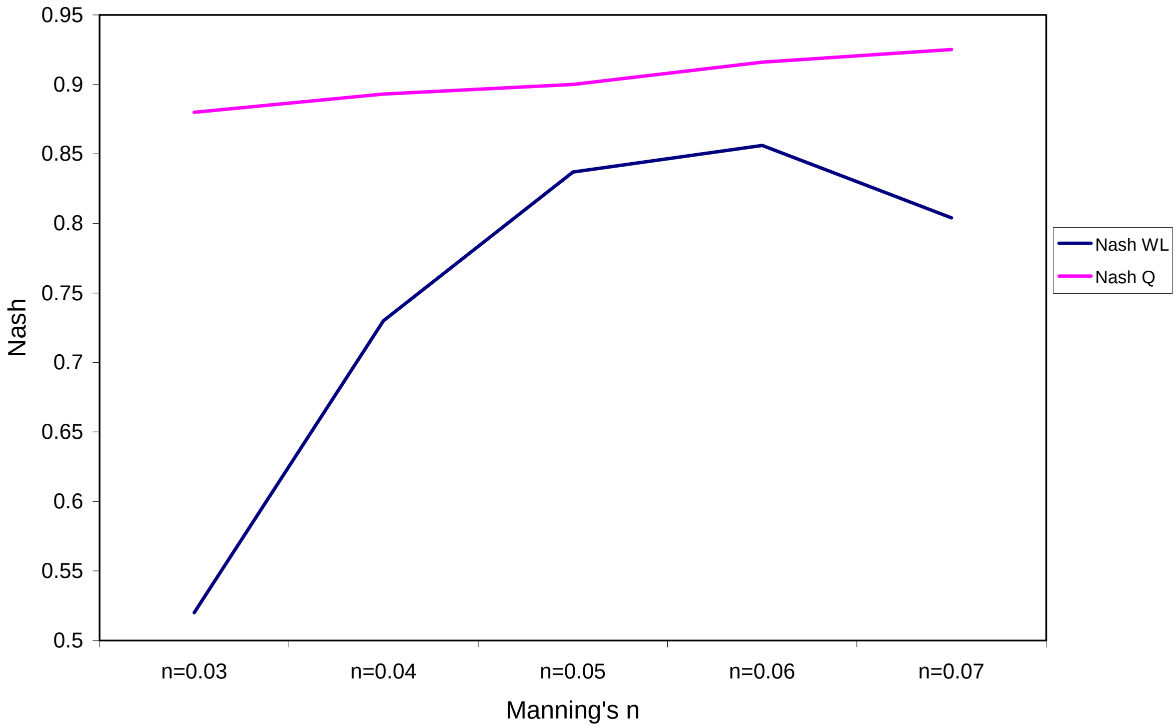

Fig. 38 Recalibration of Manning's roughness coefficient

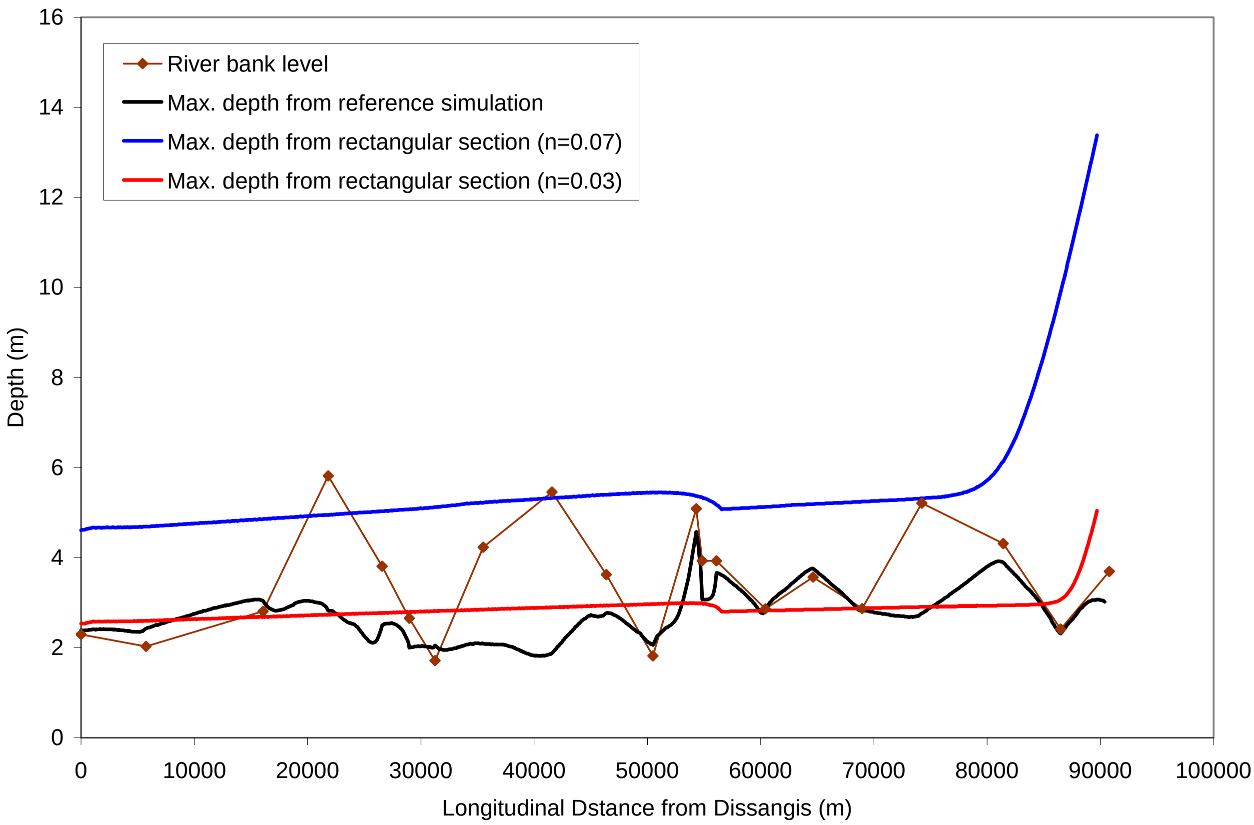

Fig. 39 Longitudinal comparison of maximum water depths along the Serein River

6.8 Scenario VIII: Excluding the floodplains from the geometry representation of the Serein River

In this scenario only surveyed main channels are used in representing the geometry of the Serein River. All floodplains are removed from the geometry representation of the river. Main channels bank walls will be extrapolated vertically once the water levels reach or overtop the river bankfull level.

The objective of this scenario is to examine the sensitivity of simulated water level peaks to the presence of floodplain (composed channel). The test also aims at identifying the attenuation in water levels of a composed channel (main channel + floodplain) compared to that obtained by only using the main channel geometry.

Table 12 illustrates the statistical comparison between the two methods at Chablis hydrometric station. The results at Chablis were slightly influenced by the removal of floodplains from the representation of the geometry. The influence was not due to the interaction between the main channel and floodplain in Chablis, because no overtopping occurred at Chablis station during the period of simulation. The slight influence on results was due to the influence of overtoppings and main channel floodplain interactions upstream and downstream from the Chablis section.

Table. 12 Nash statistical index at Chablis

Type of geometry	Nash WL	Nash Q	RMSE WL (m)	RMSE Q m^3/s
Only surveyed main channels	0.87	0.90	0.16	3.56
Surveyed main channels and floodplains	0.896	0.90	0.14	3.5

Comparison was also conducted in section 18 (located 5.8 km from Dissangis) where overtopping has been simulated in the simulation of reference. Figure 40 illustrates the comparison between the main channel and the compound channel, the figure also illustrates the attenuation of the maximum water level caused by the interaction between the main channel and floodplain.

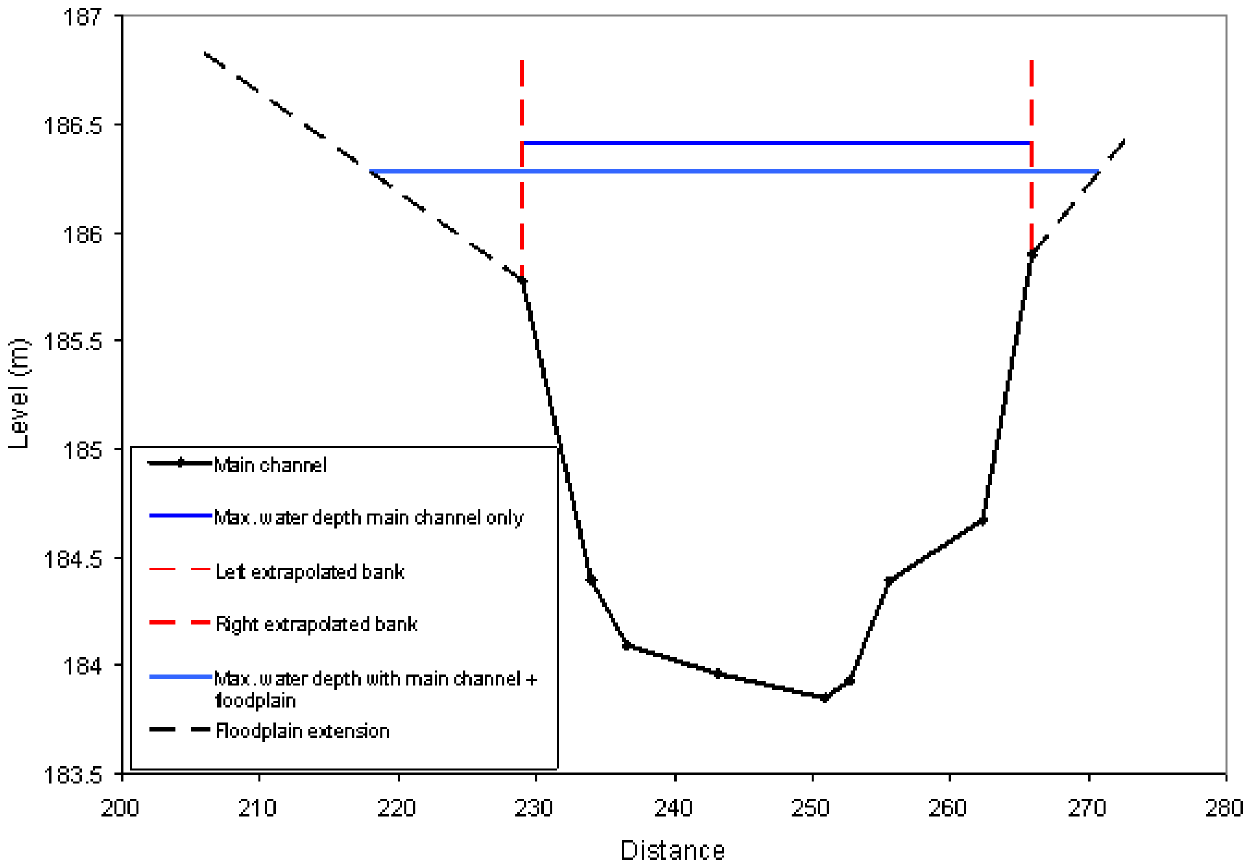

Fig. 40 Cross section 18 main channel and floodplain with maximum water levels obtained from both scenarios

Observed water level hydrographs are not available in this section so the comparison was based on comparing two simulated hydrographs; the first obtained by using only surveyed main channel geometry, while the second hydrograph was obtained using composed surveyed channels (main channels connected to floodplains).

The peak water levels of 1998 and 2001 were compared in figures 41 and 42 respectively. The comparison exhibits the obvious influence of floodplains in attenuating the peak water levels. The attenuation in the composed channel is due to the fact that when water starts overtopping from the main channel to the floodplain water starts moving laterally away from the channel, inundating the floodplain. As the depth increases, the floodplain begins to convey water downstream, generally along a shorter path that of the main channel, when the river stage is falling, water moves toward the channel from the overbank supplementing the flow in the main channel.

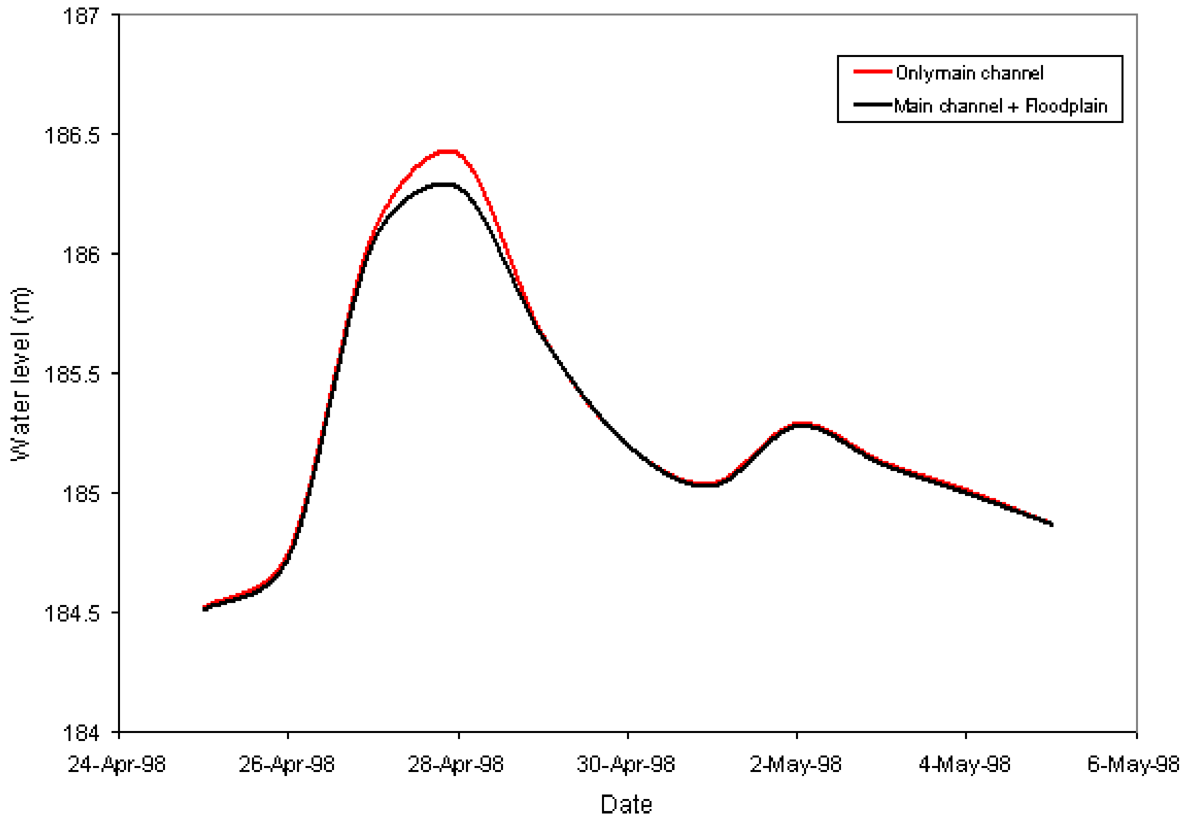

Fig. 41 Peak simulated water level of the April 1998 flood (Comparison between main channel and compound channel simulations)

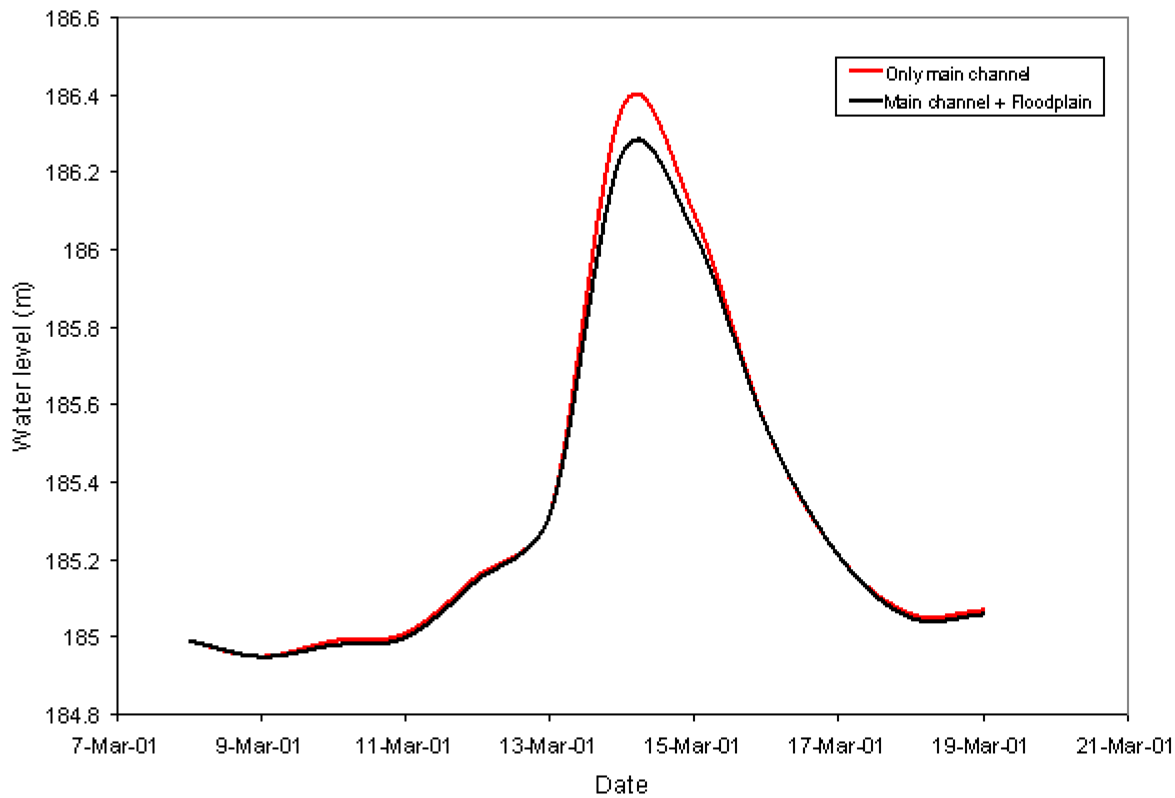

Fig. 42 Peak simulated water level of the March 2001 flood (Comparison between main channel and compound channel simulations)

Finally the maximum water depths along the river reach were longitudinally compared in order to assess the influence of floodplains on the whole river reach (figure 43). The figure shows the importance and influence of floodplains on water level attenuation whereas overtopping has occurred. To further explore the main channel and floodplain interactions more sophisticated hydraulic models should be explored in order to consider the complex physical process in this interaction such as turbulence.

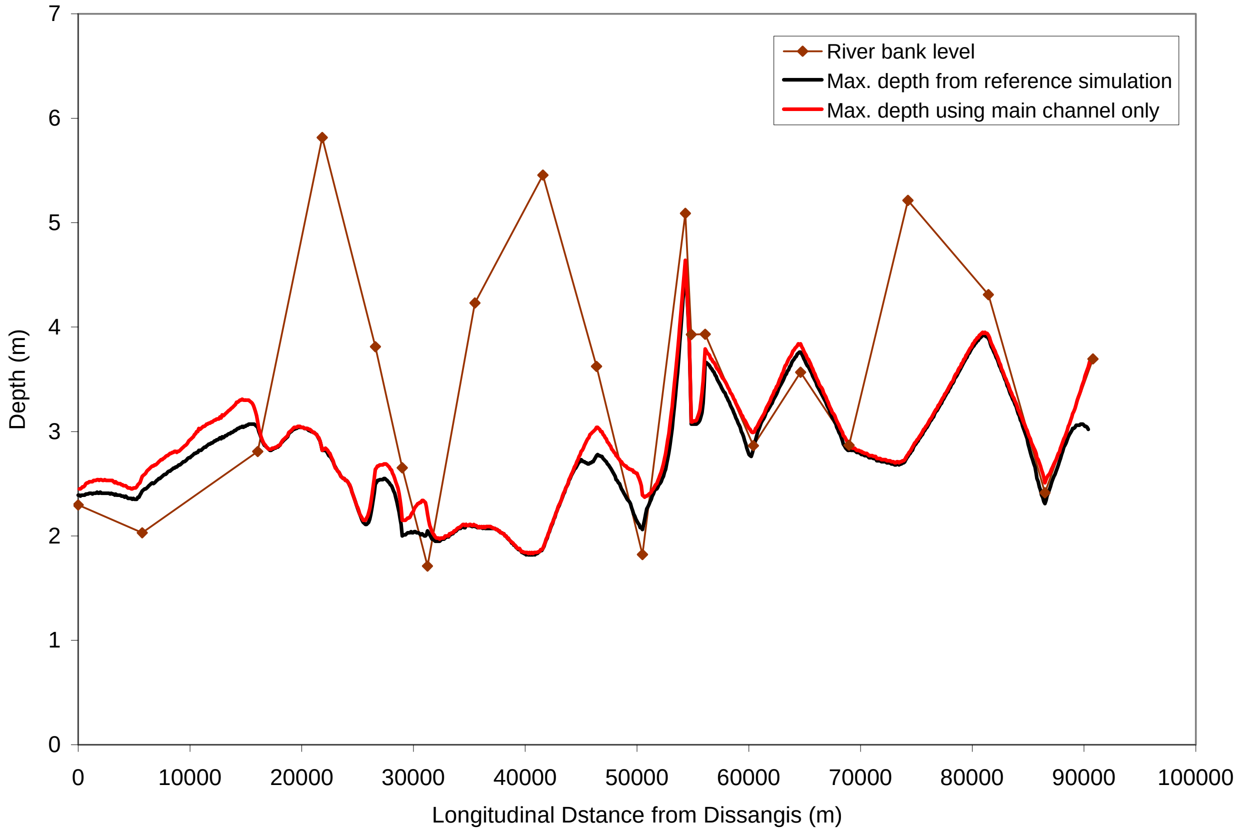

Fig. 43 Longitudinal comparison of maximum water depths along the Serein River

7 Conclusions:

The primary objective of this study was to establish whether a reliable hydraulic flood routing model could be developed based on limited field data. The validity of this approach has been illustrated by developing a model of the Serein River from Dissangis to Beaumont (confluence with the Yonne River).

The hydraulic model used is based on the Saint Venant equations which were solved using the four point implicit finite difference scheme. The calibration parameter involved in the development of the hydraulic model was the Manning's roughness coefficient (n). The lateral inflows of the Serein River subcatchments were simulated by the hydrogeological model MODCOU.

The results of this study indicate that hydraulic routing based on the Saint Venant equations could be successfully used to determine discharge hydrographs in reaches where little channel geometry data are available, by approximating the modeled reach with simplified geometry. However, a hydraulic model based on approximate channel geometry does not always predict the associated water levels. The results show that the accuracy of predicted water levels, maximum water depths rely on an accurate representation of channel geometry and bed level slopes along the river reach. Simpler forms of the Saint Venant equations (kinematic wave equation or the diffusion wave equations) should be tested in reaches where cross sections are lacking in order to explore the sensitivity of these models to geometry.

The study also illustrate the importance of accurately identifying the bankfull level where the main channel connects to the floodplain causing attenuation of water levels due to the change in the nature of flow from deep rapid flow in the main channel to shallow and slow flow in the floodplain.

In terms of calibration, the study illustrates the importance of spatial calibration in river reaches, as simulated water levels and discharges hydrographs could be accurate when compared at the control point but incorrect in other parts of the river reach. The study also illustrates the importance of calibrating to water level hydrographs and not only discharge hydrographs. This is a major difference between hydraulic and hydrological routing

8 References:

Abbott, M. B., Bathurst, J. C., Cunge, J. A., O'Connell, P. E. and Rasmussen, J., 1986, An introduction to the European Hydrological System -Système Hydrologique Européen, SHE. 2. Structure of a physically-based, distributed modeling system., Journal of Hydrology, 87-77.

Ambroise, B, Beven, K J, and Freer, J, 1996a. Towards a generalisation of the TOPMODEL concepts: topographic indices of hydrological similarity. Water Resour. Res., 32(7), 2135-2145

Ambroise, B, Freer, J and Beven, K, 1996b. Application of a generalised TOPMODEL to the small Ringelbach catchment, Vosges, France. Water Resour. Res., 32(7), 2147-2159

Ambroise, B., Perrin, J. L., and Reutenauer, D. (1995). Multicriterion validation of a semidistributed conceptual model of the water cycle in the Fecht catchment. *Water Resour. Res.*, 31(6):1467– 1481.

Andrysiak P. B. Jr. & Maidment, David, Phd (2000). "Visual Floodplain Modeling with Geographic Information Systems (GIS)". Austin Center for Research in Water Resources, the University of Texas.

Arora, V. K. and Boer, G. J.: A variable velocity flow routing algorithm for GCMs, J. Geophy. Res., 104 (D24), 30 965–30 979, 1999.

Arora, V. K., and G. J. Boer, A variable velocity flow routing algorithm for GCMs, *J. Geophys. Res*., 104, 30965-30979, 1999.

Arora, V. K., and G. J. Boer, The effect of simulated climate change on the hydrology of major river basins, accepted *J. Geophys. Res*., 2000.

Arora, V. K., F. H. S Chiew, and R. B. Grayson, A river flow routing scheme for general circulation models, *J. Geophys. Res*., 104, D12, 14347-14357, 1999.

Arora, V. K., F. H. S Chiew, and R. B. Grayson, The use of river runoff to test the CSIRO9 land surface scheme in the Amazon and the Mississippi River basins, *Intl. J. Climatology*, 20(10), 1077-1096, 2000.

Arora, V. K., Land surface modelling in general circulation models: A hydrological perspective, Ph.D. thesis, Univ. of Melbourne, Australia, 1997.

Arora, V.K., F. Seglenieks, N. Kouwen, and E. Soulis (2001) Scaling aspects of river flow routing, *Hydrological Processes*, 15(3), 461-477

Barkau, R.L., 1982, "Simulation of the July 1981 Flood Along the Salt River," Report for CE695BV, Special Problems in Hydraulics, Department of Civil Engineering, Colorado State University, Ft. Collins, CO.

Barkau, R.L., 1985, "A Mathematical Model of Unsteady Flow Through a Dendritic Network," Ph.D. Dissertation, Department of Civil Engineering, Colorado State University, Ft. Collins, CO.

Barkau, Robert L., 1992. UNET, One-Dimensional Unsteady Flow Through a Full Network of Open Channels, Computer Program, St. Louis, MO.

Bathurst, J. C., Flow processes and data provision for channel flow models, in *Modelling geomorphological systems*, M. G. Anderson Eds., Wiley, Chichester, pp 127-152, 1988.

Becker, A., and P. Serban, Hydrological models for water-resources systems design and operation, *WMO Operational Hydrology Report* No. 34, 80 pp, 1990.

Beven, K J and Kirkby, M J. 1979 A physically based variable contributing area model of basin hydrology *Hydrol. Sci. Bull*., 24(1),43-69.

Beven, K. and Kirkby, M. J. (1993). *Channel network hydrology*. John Wiley & Sons Ltd., New York.

Blench, T (1969) Mobile-bed Fluviology, University of Alberta Press, Edmonton, Canada.

Boukerma, B. (1987). Modélisation des écoulements superficiels et souterrains dans le Sud-Ouest de la France : approche du bilan hydrique. Thèse de l'Ecole Nationale Supérieure des Mines de Paris, Fontainebleau, France.

Brankensiek, D.L. 1965. An Implicit Flood Routing Method. Hydraulics Division Speciality Conference, American Society of Civil Engineers, Tucson, Arizona

Buhman, D.L., Gates, T.K., Watson, C.C., 2002. Stochastic variability of fluvial hydraulic geometry: Mississippi and Red Rivers. Hydraulic Engineering (ASCE) 128 (4), 426–437.

Cameron Ackerman. (2001)."Hydraulic Modeling of the Salt River, Arizona Using HEC-GeoRAS" Hydrologic and Hydraulic Modeling Support with GIS.

Carter, R. W., and R. G. Godfrey, Storage and flood routing, US Geological Survey Water Supply Paper, 1543-B:93, 1960.

Chang, H.H., 1988. Fluvial Processes in River Engineering. Wiley, New York, USA.

Chiu, C.-L., Lee, T.S., 1971. Stochastic simulation in study of transport processes in irregular natural streams. In: Chiu, C.-L. Calif. (Editor), Stochastic Hydraulics. Univ. of Pittsburgh, School of Engineering, Publ. Ser., 4., pp. 96-122.

Chow, V. T., *Handbook of Applied Hydrology*, pp. 7-24, McGraw-Hill, New York, 1964.

Chow, V.T., Maidment, D.R., and Mays, L.W., 1988, Applied Hydrology: New York, New York, McGraw-Hill, Inc., 572p.

Coe, M. T., N. Ramankutty, and J. A. Foley, Investigating the impact of global environmental change on terrestrial hydrological processes, *Eos Trans. AGU*, *79*(45), Fall Meet. Suppl., F359, 1998.

Coe, M., A linked global model of terrestrial hydrologic processes: Simulation of modern rivers, lakes and wetlands, *J. Geophys. Res.*, *103*, 8885-8899, 1998.

Coe, M., Simulating continental surface waters: An application to Holocene northern Africa, *J. Clim.*, *10*, 1680-1689, 1997.

Coe, M.: A linked global model of terrestrial hydrologic processes: Simulation of modern rivers, lakes and wetlands, J. Geophys. Res., 103, 8885–8899, 1998.

Cunge, J. A., On the subject of a flood propagation computation method (Muskingum Method), *J. Hydraulic Res.*, 7, 205230, 1969.

De Rose, R.C., Barrett, D., Marks, A., Caitcheon, G., Chen, Y., Simon, D., Lymburner, L., Douglas, G., Palmer, M., 2005. Regional patterns of riparian vegetation, erosion and sediment transport in the Ovens River Basin. CSIRO Land and Water Client Report, Canberra. 26 pp.

DHI Water & Environment (2001), MIKE11 Hydrodynamic Reference Manual, DHI, Horshølm, Denmark

Dingman S. L. and Sharma K. P.: Statistical development and validation of discharge equations 10 for natural channels, J. Hydrol., 1(199),13–35, 1997.

Dingman, S.L., Scharma, K.P., 1997. Statistical development and validation of discharge equations for natural channels. Journal of Hydrology 199, 13–35.

Dooge, J. C. I., W. G. Strupczewski, and J. J. Napiorkowski, Hydrodynamic derivation of storage parameters for Muskingum model, *J. Hydrol.*, 54, 371-387, 1982.

Downer, C. W., Ogden, F. L., W.D., Harmon, R. S., 2002. Theory, development and applicability of the surface water hydrologic model CASC2D. Hydrol. Processes 16, 255-275

Ducharne A, Golaz C, Leblois E, Laval K, Polcher J, Ledoux E, de Marsily G (2003). Development of a High Resolution Runoff Routing Model, Calibration and Application to Assess Runoff from the LMD GCM. Journal of Hydrology, 280: 207-228

Dunne, T., and L.B. Leopold. 1978. Water in Environmental Planning. W.H. Freeman Co. San Francisco, CA.

Dyhouse G., Hatchett J., and Benn J., Floodplain Modeling using HEC-RAS, Haestad Press, Waterbury, CT USA (2003)

Environmental Systems Research Institute Hydrologic Engineering Center (2004) "HEC GeoRAS Tools Overview Manual".

Etchevers P, Golaz C, Habets F, Noilhan J. Impact of a climate change on the Rhone River catchment hydrology. JGeophys Res 2002;107 (D16): ACL6 1-ACL6 18.

Floodplain Modeling Using HEC-RAS Author: Haestad Methods, *Gary Dyhouse*, Jennifer Hatchett, Jeremy Benn **...** Publication Date: 10/*2003*

Franchini M., Wendling J., Obled C., Todini E., 1996. Physical interpretation and sensitivity analysis of the TOPMODEL. J. Hydrol., 175, 293-338

Fread D. L., 1976, "Theoretical Development of an implicit Dynamic Routing Model," Hydrological Research Laboratory, Office of Hydrology, USDOC, NOAA, NWS, Silver Spring, MD., Presented at Dynamic Routing Seminar, Lower Mississippi River Forecast Center, Slidell, LA., 13-17 Dec 1976

Fread, D. L., Discussion of implicit flood routing in natural channels by M. Amein and C. S. Fang. J. Hydraulic Div., ASCE, 97 (HY7), 1156-1159, 1971.

Fread, D. L.: Flow Routing, in Handbook of Hydrology, edited by Maidment, D. R., McGrawHill, New York, pp. 10.1–10.36, 1993.

Fread, D.L and Lewis, J.M., NWS FLDWAY MODEL, Hydrologic Research Laboratory, Office of Hydrology, National Weather Service, NOAA, Nov. 28, 1998.

Fread. D.L., ‘Channel Routing’, Hydrological Forecasting. Edit by M.G.Anderson and T.P.Burt, 437-503, 1985.

Freeze, R.A. and Harlan, R.L. (1969). Blueprint for a physically-based digitally-simulated hydrological response model. Journal of Hydrology, 9, 237-258

GIRARD G., MORIN G. et CHARBONNEAU R., 1972. Modèle précipitation-débits à discrétisation spatiale, Cahier ORSTOM, série hydrologique, Vol IX, n°4, pp 5-52.

Golaz, C. (1999). Modélisation hydrologique a l’´echelle régionale appliquée au bassin du Rhône. Comparaison de deux modes de calcul des bilans hydriques de surface et étude de sensibilité `a une perturbation des forçages climatiques. Thèse de Doctorat de l’Ecole des Mines de Paris, Fontainebleau, France.

Gomez E, Ledoux E, Viennot P, Mignolet C, Benoit M, Bornerand C, Schott C, Mary B, Billen G, Ducharne A, Brunstein D (2003). Un outil de modélisation intégrée du transfert des nitrates sur un système hydrologique: application au bassin de la Seine. La Houille Blanche, No. 3/2003

Gomez, E. (2002). Modélisation intégrée du transfert de nitrate à l’échelle régionale dans un système hydrologique. Application au bassin de la Seine. Ph. D. thesis, Ecole Nationale Supérieure des Mines de Paris.

Gomez, E. and E. Ledoux (2001). Démarche de modélisation de la dynamique de l’azote dans les sols et de son transfert vers les aquifères et les eaux de surface. C.R. Acad. Agric. 87(1), 111–120.

Gordon, N.D., 1996. The Hydraulic Geometry of the Acheron River, Victoria, Australia. Unpublished Report by the Centre for Environmental Applied Hydrology, The University of Melbourne, Australia.

Gubala, C.P., Eilers, J.M., Bemert, J.A., 1996. The relationships between river channel morphology, complexity and aquatic habitat. Proc. 2nd IAHR Symp. Habitat Hydraulics, Ecohydraulics 2000, 1996, INRS-Eau with FQSA, IAHR, Québec, pp. B299-B306.

Harder, J.A and Armacost, L.V. 1966. Wave propogation in rivers. Hydraulic Engineering Laboratory, report No. 1, Serien 8, University of California, Berkeley

Habets, F, Gascoin, S., Korkmaz, S., Thièry, D., Zribi, M., Amraoui, N., Carli, M., Ducharne, A., Leblois, E., Ledoux, E., Martin, E., Noilhan, J., Ottlé, C. and Viennot, P. (2009). “Multi-model simulation of a major flood in the groundwater-fed basin of the Somme River (France).” *J. Geophys. Res.* [SUBMITTED].

Habets, F., J. Noilhan, C. Golaz, J. P. Goutorbe, P. Lacarrère, E. Leblois, E. Ledoux, E. Martin, C. Ottlé, D. Vidal-Madjar, 1999a: The ISBA surface scheme in a macroscale hydrological model applied to the Hapex-Mobilhy area Part 1: Model and database. *J. Hydrol.*, 217, 75-96.

Habets, F., P. Etchevers, C. Golaz, E. Leblois, E. Ledoux, E. Martin, J. Noilhan, and C. Ottlé, 1999b: Simulation of the water budget and the river flows of the Rhone basin. J. Geophys. Res.104 (D24), 31145-31172

Hagemann, S. and D¨umenil, L.: A parameterization of lateral water flow for the global scale, 25 Clim. Dyn., 14, 17–41, 1998.

Hagemann, S. and Dumenil, L.: A parameterization of lateral water flow for the global scale, 25 Clim. Dyn., 14, 17–41, 1998.

Harbaugh, A.W., Banta, E.R., Hill, M.C., and McDonald, M.G., 2000, MODFLOW2000, The U.S. Geological Survey modular ground-water model—User guide to modularization concepts and the ground-water flow process: U.S. Geological Survey Open-File Report 00-92, 121 p.

Harman C., Stewardson M., DeRose R. Variablity and uncertainty in reach bankfull hydraulic geometry. Journal of hydrology (2008) 351, 13-25

Havnø, K., Madsen, M.N., Dørge, J., 1995. MIKE11, a generalized river modeling package. In: Singh, V.P., (Ed.), Computer Models of Watershed Hydrology, Water Resources Publications, Englewood, USA, pp. 733–782.

HEC-GeoRAS; an extension for support of HEC-RAS using Arcview Users manual, Version 3.0, U.S. Army Corps of Engineers Hydrologic Engineering Center, Davis, California, April 2000.

Hey, R.D., Thorne, C.R., 1986. Stable channels with mobile gravel beds. Journal of Hydraulic Engineering, ASCE 112 (8), 671–689.

HR WALLINGFORD (1997), ISIS user reference manual, HR Wallingford, Wallingford, OXON

J. J. Stoker, Water waves: The mathematical theory with applications, Pure and Appl. Math., vol. 4, Interscience, New York, 1957.

Jobson, H.E. et Harbaugh, A.W., 1999, Modifications to the Diffusion Analogy Surface-Water Flow Model (DAFLOW) for Coupling to the Modular Finite-Difference Ground-Water Flow Model (MODFLOW), U.S. Geological Survey Open-File Report 99-217, 107 p.

Johnson, P.A., and T.M. Heil. 1996. Uncertainty in Estimating Bankfull Conditions. Water Resources Bulletin. Journal of the American Water Resources Association 32(6):1283-1292.

Johnson, P.A., and T.M. Heil. 1996. Uncertainty in Estimating Bankfull Conditions. Water Resources Bulletin. Journal of the American Water Resources Association 32(6):1283-1292.

Jowett, I.G., 1998. Hydraulic geometry of New Zealand rivers and its use as a preliminary method of habitat assessment. Regulated Rivers: Research and Management 14, 451–466.

Julien, P Y and Wargadalam, J (1995) "Alluvial channel geometry: Theory and applications", J Hydraulic Engineering, Volume 121.

Julien, P. Y., et al. (1995), Raster-Based Hydrologic Modeling of Spatially-Varied Surface Runoff, *Water Resources Bulletin*, *31*, 523-536.

Kilpatrick, F.A., and H.H. Barnes Jr. 1964. Channel Geometry of Piedmont Streams as Related to Frequency of Floods. Professional Paper 422-E. US Geological Survey, Washington, DC.

Kilpatrick, F.A., and H.H. Barnes Jr. 1964. Channel Geometry of Piedmont Streams as Related to Frequency of Floods. Professional Paper 422-E. US Geological Survey, Washington, DC.

Knebl, M. R., et al. (2005), Regional scale flood modeling using NEXRAD rainfall, GIS, and HEC-HMS/RAS: a case study for the San Antonio River Basin Summer 2002 storm event, Journal of Environmental Management, 75, 325-336.

KNIGHT D W (2001), Conveyance in 1-D river models, Expert Review Paper, Annex to final report on Environment Agency R&D project "Scoping Study for Reducing Uncertainty in River Flood Conveyance", Environment Agency, Bristol.

Knighton, D. 1984. Fluvial Forms and Process. Edward Arnold, London.

Knudsen, J., A.Thomsen, and J. C. Refgaard, WATBAL. A semi-distributed, physically based hydrological modeling system, Nordic Hydrol., 17, 347-362, 1986

Lacey, G (1929) "Stable channels in alluvium" Min. Proc. Institution of Civil Engineers, London, Volume 229.

Lamouroux, N., Capra, H., 2002. Simple predictions of instream habitat model outputs for target fish populations. Freshwater Biology 47 (8), 1543–1556.

Lamouroux, N., Suchon, Y., 2002. Simple predictions of instream habitat model outputs for habitat guilds in large streams. Freshwater Biology 47 (8), 1531–1542.

Ledoux E et al. Agriculture and groundwater nitrate contamination in the Seine basin. The STICSmodelling chain. Sci Total Environ (2007), doi:10.1016/j.scitotenv.2006.12.002

Ledoux E, Girard G, de MarsilyG, Villeneuve JP, Deschenes J. Spatially distributed modeling: conceptual approach, couplingsurface water and groundwater. In: Morel-Seytoux HJ, editor. Unsaturated flow in hydrologic modeling — theory and practice. NATO ASI Ser. CNorwell, Massachussett: Kluwer Academic; 1989 . p. 435–54.

Ledoux E, Girard G, Villeneuve JP. Proposition d'un modèle couplé pour la simulation conjointe des écoulements de surface et des écoulements souterrains sur un bassin hydrologique. La Houille Blanche; 1984 . p. 101–10.

Ledoux, E., et al. (1989), *Spatially distributed modeling: conceptual approach, coupling surface water and groundwater, in Unsaturated Flow in Hydrologic Modeling Theory and Practice,* edited by H. J. Morel660 Seytoux, Kluwer Academic Publishers.

Ledoux, E., Modélisation intégrée des écoulements de surface et des écoulements souterrains sur un bassin hydrologique. Ph.D. thesis, Ecole des Mines, 1980.

Leopold and Maddock, 1953 L.B. Leopold and T. Maddock, The hydraulic geometry of stream channels and some physiographic implications, *U.S. Geological Survey Paper* 252 (1953), pp. 1–57.

Leopold et al., 1964 L.B. Leopold, M.G. Wolman and J.P. Miller, Fluvial Processes in Geomorphology, W.H. Freeman and Company, San Francisco (1964) 522 pp.

Leopold, L.B. (1994). A view of the River. Harvard University Press, Cambridge, Massachusetts.

Leopold, L.B., 1994. A view of the River. Harvard University Press, Cambridge, Massachusetts.

Leopold, L.B., Maddock, T., 1953. The hydraulic geometry of stream channels and some physiographic implications. United States Geological Survey, 1–57.

Leopold, L.B., Wolman, M.G., et al., 1964. Fluvial Processes in Geomorphology. W.H. Freeman, San Francisco, California, USA.

Liggett, J. A., Basic equations of unsteady flow, in Unsteady Flow in Open Channels, K. Mahmood, and V. Yevjevick (Eds.), Vol. I, Fort Collins, Colorado,Water Resources Publications, pp. 29-62, 1975.

Lindley, E S (1919) “Regime channels”, proc. Punjab Engineering Congress, Volume 7.

Linsley, R.K. 1971. A critical riview of currently avaiolable hydrological model for ananlysis of urban stormwater runoff. Report, Hydrocomp International Inc., Palo Alto, California

Lt, S. G., Venkataraman, L., McLaughlin, D., 1992. Stochastic theory for irregular modeling, Part 1. Flow resistance. J. Hydraul. Eng. 118, 1079-1089

Lu, H., Moran, C.J., Prosser, I.P., De Rose, R., 2004. Investment prioritization based on broad scale spatial budgeting to meet downstream targets for suspended sediment loads. Water Resources Research 40, W09501. doi:10.1029/2003WR002966

M. J. Lighthill et G. B. Whitham, *On kinematic waves. I. Flood movement in long rivers*, Proceedings of the Royal Society of London, Piccadilly, London, 10 May 1955, A229 (1178):281–316

Maddock, T (1970) “Intermediate hydraulics of alluvial channels”, J Hydraulics Divn., ASCE, Volume 96.

Matt M., Pater W., 2006. An application of the distributed hydrologic model CASC2D to a tropical montane watershed. Journal of Hydrology 330, 481 - 495

McKergow, L.A., Prosser, I.P., Hughes, A.O., Brodie, J., 2004. Sources of sediment to the Great Barrier Reef World Heritage Area. Marine Pollution Bulletin 51, 200–211.

Merritt, M.L., and Konikow, L.F., 2000, Documentation of a computer program to simulate lake-aquifer interaction using the MODFLOW ground-water flow model and the MOC3D solute-transport model: U.S. Geological Survey Water-Resources Investigations Report 00-4167, 146 p.

Miller B.A. and Wenzel H.G., 1984. Low flow hydraulics in alluvial channels Jr., Dept. of Civil Engineering, University of Illinois at Urbana-Champaign.

Miller, J. R., and G. L. Russell, The impact of global warming on river runoff, *J. Geophys. Res.*, 97, 2757-2764, 1992.

Miller, J. R., G. L. Russell, and G. Caliri, Continental-Scale river flow in climate models, *J. Clim.*, 7, 914-928, 1994.

Milly, P. C. D., Dunne, K. A., and Vecchia, A. V.: Global pattern of trends in streamflow and water availability in a changing climate, Nature, 438(7066), 347–350, 2005.

Nash JE, Sutcliffe JV. River flow forecasting through conceptual models, 1. A discussion of principles. J Hydrol 1970;10: 282–90.

Ngo-Duc, T., et al. (2007), A variable streamflow velocity method for global riverrouting model: model description and preliminary results, *Hydrol. Earth Syst. Sci.Discuss.*, *4*, 4389-4414.

Niswonger, R.G., and Prudic, D.E., 2005, Documentation of the Streamflow-Routing (SFR2) Package to include unsaturated flow beneath streams—a modification to SFR1: U.S. Geological Survey Techniques and Methods Book 6, Chap. A13, 57 p.

Nixon, M. 1959. A Study of Bankfull Discharges of Rivers in England and Wales. In Proceedings of the Institution of Civil Engineers, vol. 12, pp. 157-175.

Ogden, F.L., 1994, de St. Venant Channel Routing in Distributed Hydrologic Modeling, Proc. ASCE Hydraulic Engineering Specialty Conference, Buffalo, N.Y., August 1-5.

Ogden, F.L., 1997, CASC2D Reference Manual, Dept. of Civil & Environmental Engineering, U-37, University of Connecticut, Storrs, CT 06269, 106 pp.

Ogden, F.L., and P.Y. Julien, 1994, Runoff model sensitivity to radar rainfall resolution, *J. Hydrology*, Vol. 158, pp. 1-18.

Ogden, F.L., and S.U.S. Senarath, 1997, Continuous Distributed Parameter Hydrologic Modeling with CASC2D, Proc. XXVII Congress, International Association of Hydraulic Research, San Francisco, CA, Aug. 10-15.

Ogden, F.L., S.U.S. Senarath, and B. Saghafian, 1998, Use of Continuous Simulations to Improve Distributed Hydrologic Model Calibration Uniqueness, *in preparation*.

Oki, T. and Kanae, S.: Global Hydrologic Cycle and World Water Resources, Science, 313, 5790, 1068–1072, doi:10.1126/science.1128845, 2006.

Oki, T. and Sud, Y. C.: Design of Total Runoff Integrating Pathways (TRIP) – A global river channel network. Earth Interactions 2., available at http://EarthInteractions.org, 1998.

Pappenberger, F., Beven, K.J., Horritt, M. and Blazkova, S., 2005. Uncertainty in the calibration of effective roughness parameters in HEC-RAS using inundation and downstream level observations. Journal of Hydrology, 302(1-4): 46-69

Prosser, I.P., Rustomji, P., Young, W., Moran, C.J., Hughes, A.O., 2001a. Constructing river basin sediment budgets for the national land and water resources audit. CSIRO Land and Water Tech. Report no 15/01. CSIRO Land and Water, Canberra.

Prosser, I.P., Rutherfurd, I.D., Olley, J.M., Young, W.J., Wallbrink, P.J., Moran, C.J., 2001b. Large-scale patterns of erosion and sediment transport in river networks, with examples from Australia. Marine and Freshwater Research 52, 81–99.

Prudic, D.E., Konikow, L.F., and Banta, E.R., 2004, A new Streamflow-Routing (SFR1) Package to simulate stream-aquifer interaction with MODFLOW-2000: U.S. Geological Survey Open-File Report 2004-1042, 95 p.

Rabeni, C.F. and Jacobson, R.B., 1993, Geomorphic and hydraulic influences on the abundance and distribution of stream centrarchids in Ozark U.S.A. streams**:** Polskie Archiwum Hydrolobiologii, v. 40, p. 87-99.

Rabeni, C.F., and Jacobson, R.B., 1993, The importance of fluvial hydraulics to fish-habitat restoration in low-gradient alluvial streams**:** Freshwater Biology, v. 29, p. 211-220.

Refsgaard J.C and Knudsen J (1996) Operational validation and intercomparison of different types of hydrological models, Water Resources Research, 32: (7), 2189-2202

Refsgaard, J. C., and B. Storm (1995), MIKE SHE, in *Computer Models of Watershed* 708 *Hydrology*, edited by V. P. Singh, pp. 809-846, Water Resources Publications, Highlands 709 Ranch, CO, USA.

Richard Kraus.(2000)."Floodplain Determination Using ArcView GIS & HEC-RAS." Hydrologic and Hydraulic Modeling Support with GIS.

Richards, K.S., 1982. Rivers, Form and Process in Alluvial Channels. Methuen, New York, USA.

Sahoo, G. B., et al. (2006), Calibration and validation of a physically distributed hydrological model, MIKE SHE, to predict streamflow at high frequency in a flashy mountainous Hawaii stream, *Journal of Hydrology*, *327*, 94-109.

Schulze, K., Hunger, M., and Doll, P.: Simulating river flow velocity on global scale, Adv. Geosci., 5, 133–136, 2005.

Schumm, S.A., (1960) The shape of alluvial channels in relation to sediment type: U.S. Geol. Survey Prof. Paper 352-B, p. 17-30

Shen, H.W., et Julien, P.Y., 1993, Erosion and sediment transport, in Maidment, D.R., ed., Handbook of Hydrology: New York, McGraw-Hill, Inc., p.61.

Sherman, L. K., Stream-flow from rainfall by the unit-graph method, *Eng. News-Rec*., 108, 501-505, 1932.

Simons, D B and Albertson, M L ("Uniform water conveyance channels in alluvial material", Trans. ASCE, Volume 128.

Singh, K.P. and McConkey, S. (1989). Hydraulic geometry of streams and stream habitat assessment. Journal of Water Resources Planning and Management 115: 583-597.

Singh, K.P., McConkey, S., 1989. Hydraulic geometry of streams and stream habitat assessment. Journal of Water Resources Planning and Management 115 (5), 583–597.

Smith, R.H., 1978, "Development of a Flood Routing Model for Small Meandering Rivers," Ph.D. Dissertation, Department of Civil Engineering, University of Missouri at Rolla, MO.

Smith, R.H., 1978, "Development of a Flood Routing Model for Small Meandering Rivers," Ph.D. Dissertation, Department of Civil Engineering, University of Missouri at Rolla, MO.

Snell, J. D. and M. Sivapalan (1995). On the application of the meta-channel concept: Construction of the meta-channel hydraulic geometry for a natural catchment. Hydrological Processes, Vol. 9, Nos. 5/6, pp. 485-505.

Stewardson M., 2005. Hydraulic geometry of stream reaches. Journal of Hydrology 306 (2005) 97–111

Stewardson, M, DeRose. R., and Harman. C., (2005). Regional models of stream channel metrics, Technical report. Cooperative Research Centre for Catchment Hydrology, Melbourne University, Australia.

Stewardson, M.J., McMahon, T.A., 2002. A stochastic model of hydraulic variation in stream reaches. Water Resources Research 38 (1), 8. 1–14.

Tatum, F.E. 1940. A simplified method of routing flood flows through natural valley storage. Unpublished memorandum, US. Engineers Office, Rock Island, Illinois.

Thompson, J. R., et al. (2004), Application of the coupled MIKE SHE/MIKE 11modelling system to a lowland wet grassland in southeast England, *Journal of Hydrology*, *293*, 151-179.

US Army Corps of Engineers (2002), HEC-RAS River Analysis System, Hydraulic Reference Manual, USACE Hydrologic Engineering Center, Davis CA.

Wang, X., P. H. Stone, and J.. Marotzke, Global thermohaline circulation. Part I – Sensitivity to atmospheric moisture transport, *J. Clim*., 12, 71-82, 1999.

Weinmann, P. E., and E. M. Laurenson, Approximate flood routing methods: A review, *J. Hydraulic Div*., ASCE, 105 (HY13), Proc., Paper 15057, 1979.

Western, A.W., Finlayson, B.L., et al., 1997. A method for characterising longitudinal irregularity in river channels. J. Geomorphology 21, 39–51.

Wijffels, S.E., R.W. Scimtt, H.L. Bryden and A. Stigebrandt. 1992. On the transport of freshwater by the oceans, *J. Phys. Oceanogr*., 22, 155-162

Wilkinson, S., Henderson, A., Chen, Y., (2004). SedNet User Guide, A CSIRO land and Water client report for the Cooperative Research Centre for Catchment Hydrology, Australia.

Williams, G.P. 1978. Bank-full discharge of rivers. Water. Res. 14(6):1141-1154.

Wilson, E. M., *Engineering Hydrology*, pp. 110, 196, and 301, Macmillan, Indianapolis, Indiana, 1990.

9 Acknowledgments:

We would like to thank the centre National des Œuvres Universitaires et Scolaires and the Programme Interdisciplinaire de Recherche sur l'Environnement for financing this thesis. We would also like to thank the Direction Régionale de l'Environnement - DIREN - Ile de France for providing the necessary morphological and hydrological data for the Serein Model.